IEEE Access
Multidisciplinary | Rapid Review | Open Access Journal

Received 26 August 2025, accepted 19 October 2025, date of publication 30 October 2025, date of current version 6 November 2025.

Digital Object Identifier 10.1109/ACCESS.2025.3626696

TOPICAL REVIEW

Review of Smartphone Deep Learning Applications Using Eye Imaging Diagnostic Techniques in Ophthalmology

V. KURILOVA[1,2,3], J. GOGA[1], A. THURZO[4], J. PAVLOVICOVA[1], M. ORAVEC[1], P. KOLAR[2,3], AND N. MAJTANOVA[2,3]

[1]Faculty of Electrical Engineering and Information Technology, Slovak University of Technology, 812 19 Bratislava, Slovakia
[2]Department of Ophthalmology, University Hospital in Bratislava, Slovak Medical University in Bratislava, 851 07 Bratislava, Slovakia
[3]Faculty of Medicine, Slovak Medical University in Bratislava, 833 03 Bratislava, Slovakia
[4]Department of Orthodontics, Regenerative and Forensic Dentistry, Faculty of Medicine, Comenius University in Bratislava, 812 50 Bratislava, Slovakia

Corresponding authors: N. Majtanova (nora.majtanova@gmail.com) and V. Kurilova (veronika.kurilova@stuba.sk)

This work was supported in part by Agentúra na podporu výskumu a vývoja (APVV) through AI Supported Diagnostics in Ophthalmology under Grant APVV-22-606-AI4EYE, and in part by the AIDabiomeDIA–AI in Development of Advanced Biometrics and Medicine Diagnostics under Grant Vedecká grantová agentúra (VEGA) 1/0202/23.

ABSTRACT Eye diseases, which often lead to severe vision loss, can be prevented, reversed, or slowed down if diagnosed early. The demand for accurate and timely diagnosis has stimulated the exploration of innovative diagnostic techniques, including the connection of deep learning with smartphone applications to analyze eye images. This review explores how smartphone-based systems transform diagnostic processes using built-in cameras, computational resources, and deep learning models to provide inexpensive solutions for early detection on a massive scale. We provide a comprehensive analysis of recent advances in smartphone deep learning applications using eye imaging diagnostic techniques in ophthalmology, highlighting the key application areas and examining the underlying methodologies, hardware, and software solutions used, as well as their clinical implications. We describe 26 complete diagnostic solutions consisting of the smartphone application with the ability to capture images using the smartphone and the accessible deep learning model, supplemented with 48 partial solutions. The aim of this review is to present an overview of current solutions and provide a comprehensive view of future directions for technicians and ophthalmologists in this emerging interdisciplinary research field.

INDEX TERMS Deep learning, mobile, neural networks, ophthalmology, smartphone, image.

I. INTRODUCTION

The leading causes of blindness and severe vision loss worldwide are cataracts, uncorrected refractive errors, glaucoma, age-related macular degeneration (AMD), and diabetic retinopathy (DR) with diabetic macular edema (DME) [1]. Some of these conditions are preventable or reversible, and their progression may be slower when diagnosed and treated early [2], [3]. Therefore, there is a need to increase available ophthalmologic care to avoid increasing global visual impairment [1]. Simple and automatic screening, diagnosis, and monitoring methods for sight-threatening conditions using artificial intelligence could be valuable [4].

Standard ophthalmologic examinations have limited accessibility and are available exclusively to healthcare professionals with the necessary medical equipment. In contrast, the worldwide penetration of smartphones was estimated to be 78% in 2020 [5]. The analysis of ophthalmic imaging requires experienced medical professionals, who are in short supply in developing countries [6]. Imaging through smartphones combined with a diagnostic computational model for ophthalmic applications can aid in earlier diagnosis without requiring highly skilled medical professionals [7]. Direct smartphone images of the anterior segment of the eye captured without any attachment could be clear and comparable in quality

The associate editor coordinating the review of this manuscript and approving it for publication was Hang Shen.

to those acquired by a standard camera. In addition to direct smartphone-captured images, capturing images using various smartphone attachments helps to obtain other types of ophthalmic images, such as slit lamp or fundus images, depending on the type of attachment used. These attachments are made to be compatible with smartphones [8], and their small size, along with smartphone features, allows some of them to capture images without the need for an examination room or immediate access to electricity and the Internet [9], [10]. Capturing fundus using these attachments or with a twenty dioptries (20D) lens alone requires both hands of a skilled examiner, a well-dilated pupil, and a cooperating patient. The field of view is limited compared to the standard fundus camera [11], [12], and inexperienced users could expect difficulties in adjusting the filming distance and glare in the lens [13]. However, the properties and functionality of smartphones vary from device to device [14]. Different possibilities offer portable handheld fundus cameras connected to smartphones; the examination technique is definitely easier, the quality of the image tends to be comparable to standard fundus cameras with lower resolution, and the field of view is usually wider compared to the smartphone with fundus attachment alone [15]. Some solutions include a non-mydriatic mode, which is made possible by multiple illumination sources using white and near-infrared (NIR) light [16].

When dealing with fundus examinations in low-income countries, buying a standard fundus camera could be expensive; moreover, such cameras are relatively large and difficult to move [8]. Smartphones with attached fundus cameras or portable smartphone-based ophthalmoscopes are practical ''on the go'' and as a useful screening tool in a general practitioner's office [17], [18]. The role of smartphones in the assessment of healthcare has been even more highlighted during the COVID-19 pandemic [19]. Smartphone-based diagnostic solutions are compact, easy to use, and usually inexpensive [20], perfectly suited for ophthalmology screening purposes, as well as for creating second opinions for clinical decision-making, assisting patients, or educational purposes. Capturing smartphone images in ophthalmology has a high potential for telemedicine solutions to increase accessibility to ophthalmic care where specialists are lacking or unavailable. Such telemedicine solutions or solutions captured using handheld cameras are widely developed and adopted [17], [21], [22] and could work with or without the implementation of artificial intelligence, including deep learning (DL).

According to recent studies, deep learning applications are suitable for use in modern ophthalmology and are expected to become standard practice in the near future [23], similar to deep learning applications in other medical subfields [24]. Advanced artificial intelligence algorithms have already been widely used for screening for various ophthalmologic diseases and in clinical decision support systems [23], [25].

We reviewed smartphone deep learning applications with eye imaging techniques in ophthalmology used for screening of various diseases, focusing on capturing eye images using smartphones, the datasets used, deep learning models, and their implementations. This review was intended to allow medical technicians and ophthalmologists to become more familiar with this novel interdisciplinary research field and its clinical meaning. To the best of our knowledge, this is the first recent review of smartphone deep learning applications using eye imaging techniques in ophthalmic disease screening in this field. Although this article review was meant to describe complete smartphone deep learning solutions in ophthalmology, including smartphone image capture techniques, deep learning model training, and its implementation in smartphone applications, we found in the literature only a limited number of these; therefore, we also include partial solutions in this review. Moreover, most of these solutions were created for scientific purposes only and could not be downloaded from Google or Apple stores. Because of that, we believe that in this growing field of research, it is also important to analyze partial solutions, which could be helpful for further research.

The remainder of the review article consists of the Methods section, with a description of the selection process and analysis of reviewed articles, followed by the Results section, where we describe the conventional examination and diagnostic process in ophthalmology versus AI-empowered smartphone imaging, the used datasets and deep learning models including their implementation in the form of smartphone applications, and the clinical benefit of these solutions. Finally, the Discussion, Future Work, and Conclusion sections are presented.

II. METHODS

Searching through the Web of Science online library, PubMed, and IEEE Xplore were used to search full-text articles in the English language from January 2, 2024, up to March 16, 2024, to find the most recent research. We searched for the combination of keywords listed in Figure 1. After searching for all combinations in all three databases, 1621 articles were indexed and manually reviewed. As the first step, we removed all duplicates from the remaining 1463 articles and selected 74 articles based on inclusion and exclusion criteria. We excluded articles mentioning deep learning only as a future research goal and articles that do not focus on the evaluation of non-image data in ophthalmology or image data of the eye, which cannot be captured nowadays by smartphones, e.g., images from optical coherence tomography (OCT). In relation to our topic, we defined that the workflow of the complete solution must contain three mandatory parts. The first stage involves using a smartphone to capture images, the second stage involves using a trained deep learning model, and the final stage involves the development of a smartphone application.

With regard to the target eye structure, the authors could capture the anterior or posterior segment of the eye. In the anterior segment are the cornea, iris, ciliary body, and lens, including aqueous humor. The posterior segment of the eye

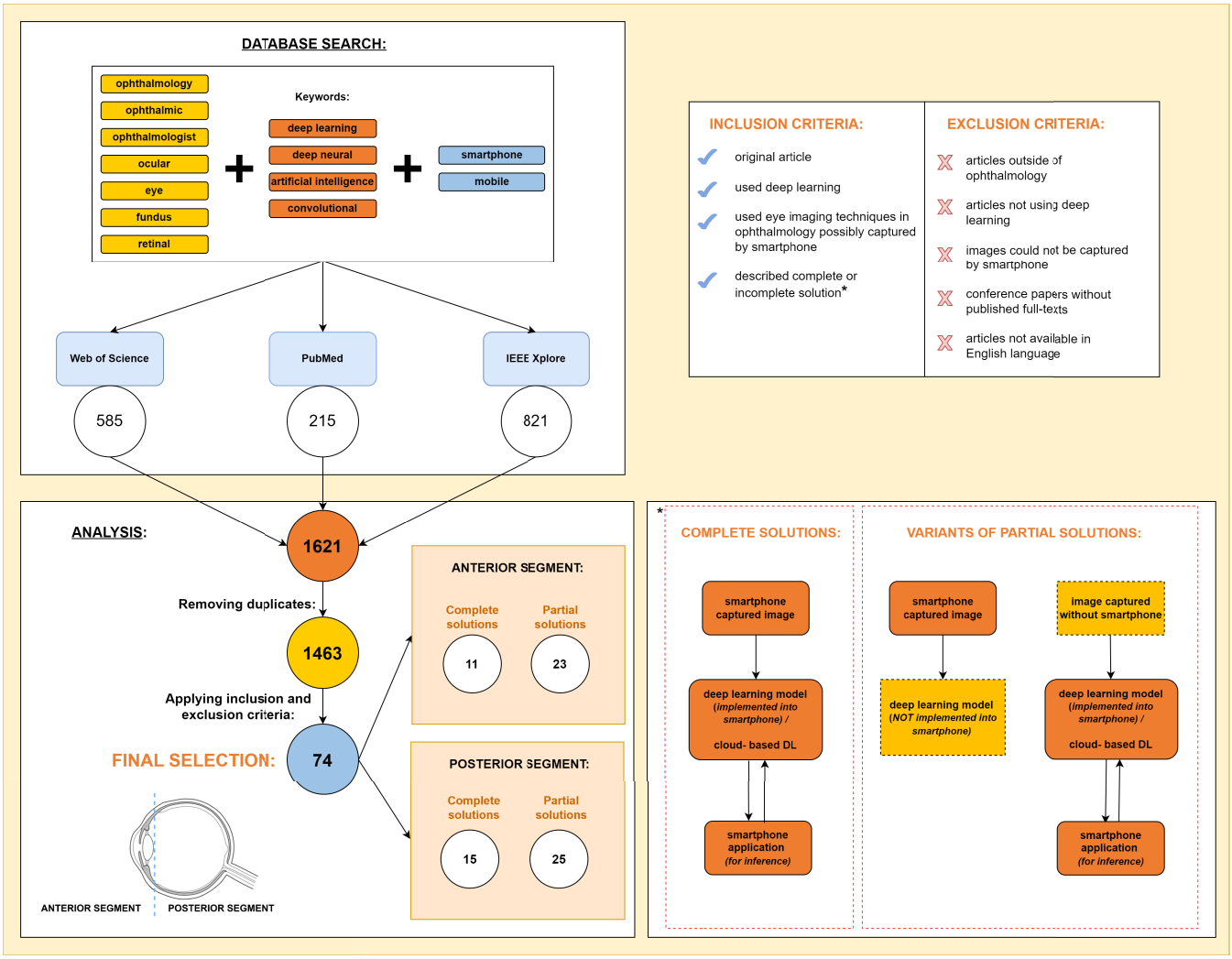

FIGURE 1. Workflow of database search and analysis, including a combination of search keywords and description of complete and partial solutions.

is composed of the retina, choroid, vitreous, and optic nerve head. It must be noted that not all structures are visible in captured photography.

The images captured on a smartphone could be used for training or testing, so we also included works in which the authors trained a deep learning model on images that were not captured using a smartphone, followed by testing the model on smartphone images. We analyzed partial solutions in two distinct categories: those designed specifically for smartphone capture but not implemented as a phone app; and those potentially using non-smartphone data sources (like public datasets or fundus camera images) where the model was actually deployed, either locally on a smartphone or via cloud-based deep learning. We think that these partial solutions could also contain valuable information to contribute to this research topic. The workflow of database search and analysis that includes the combination of search keywords and the description of complete and partial solutions is depicted in Figure 1. The final selection of the articles contains 34 anterior and 40 posterior segment solutions, respectively, primarily published in the last five years. We extracted and divided the detailed functionalities after an advanced analysis of the described applications. The selection of the research articles was performed by three independent researchers, and the resulting selections were then combined. Data extraction was performed by two independent researchers, with a third researcher verifying the results. The third researcher verified the accuracy of the results and solved the discrepancies in the opinions of the first two researchers. In this process, the specialist ophthalmologist helped solve medical-oriented and technical issues.

We reviewed the articles in full text to obtain the following data: authors, title, year of publication, main purpose of the application, image type, platform, used datasets, used deep learning architecture and their results, used hardware, source code availability, and assumed price of the solution. A brief summarization of the data of the anterior segment

TABLE 1. The evaluation score criteria.

Criterion	Tripod- AI alignment
Is the model described?	reporting of the model
Is the solution available or shared?	sharing and reproducibility
Are multiple institutions involved in the research?	external validation and generalizability
Did the authors use some public dataset for training or testing?	reproducibility
Did the authors use smartphone-captured images?	no, domain-specific
Were the images captured under constrained conditions?	reproducibility
Did the authors develop a smartphone application for inference?	no, domain-specific

The evaluation score was calculated as a sum of points for every fullfield criterion with a minimum of 0 and a maximum of 7 points.

solutions is given in Tables 2 and 3 for complete and partial solutions, respectively. The data from the posterior segment solutions are listed in Tables 4 and 5, for complete and partial solutions, respectively. In each of the first four tables, there is information for every solution image data source, disease, neural network backbone, target operating system, whether the solution contains the model description, whether the solution is online or offline, and whether it uses smartphone images for training and testing.

We assessed the quality of the reviewed articles using criteria derived from the Tripod-AI framework [26], explicitly adapted to our context, and summarized the results using an evaluation score. Our adaptation focused on model description, transparency, data sharing/reproducibility, multi-institutional validation, and crucially, the use of smartphone-captured images and the development of associated apps – areas where standard Tripod-AI was not specific enough. We evaluated the articles according to seven selected criteria (Table 1), each worth 1 point. The range of points gained was from a minimum of 0 to a maximum of 7, with four levels of evaluation score: basic (0-1 points, black color), moderate (2-3 points, orange color), good (4-5 points, yellow color), and excellent (6-7 points, blue color). Color-coded evaluation scores are presented in Tables 2 to 5.

Additional information, including the datasets used, the main task of the best-performing neural networks, and their results, is listed in Appendix Tables 8-11. Source code availability, used hardware, and price range are listed in Appendix Tables 12- 15. In both Appendix Table groups, the data are sorted in the following order: anterior complete, anterior partial, posterior complete, and posterior partial.

III. RESULTS

The Results section is composed of six subsections. The first subsection presents a conventional ophthalmological examination, followed by AI-empowered smartphone imaging in ophthalmology, subsections on datasets, preprocessing, and augmentation, deep learning models, their deployment, and, finally, a subsection describing the clinical contribution of such solutions.

A. CONVENTIONAL EXAMINATION AND DIAGNOSTIC PROCESS IN OPHTHALMOLOGY

The conventional diagnostic process for an ophthalmologic patient involves evaluation through various ophthalmic examinations, including the use of different devices. In addition to direct examination of the patient's eye, a fundamental part of the examination is ophthalmoscopy in the slit lamp. In the slit lamp, the anterior segment of the eye is examined using full light spread directly, or using the beam of light with variable height (e.g., slit beam) from different angles, or indirectly with retroillumination, when the light is reflected from the posterior structures. The posterior segment examination, including the fundus, is also performed on the slit-lamp, with the magnifying lens held in front of the patient's eye, most often after pupil dilation with mydriatic eye drops. Another option for fundus examination is to use a handheld direct ophthalmoscope or a fundus camera, a device that captures images with a built-in camera, with the option to print and save images. After summarizing the examination findings, the ophthalmologist considers the diagnosis to recommend the appropriate treatment.

When examining fundus in low-income countries, purchasing a standard fundus camera can be expensive; moreover, such cameras are relatively large and difficult to transport [8]. Therefore, handheld fundus cameras and smartphone solutions are in high demand. After summarizing the examination findings, the ophthalmologist considers the diagnosis to recommend the appropriate treatment.

B. AI-EMPOWERED SMARTPHONE IMAGING IN OPHTHALMOLOGY

We can divide smartphone eye imaging into two categories from the clinical point of view – capturing images of the anterior and posterior segment of the eye (see the lower left corner of Fig.1).

In the anterior segment imaging, images could usually be captured without any add-on hardware, except in some specific cases, which we will describe later in the text. Images of the anterior segment can be captured by the patient himself with the front camera or by another person with the rear camera [32].

Posterior segment imaging is the visualization of the fundus, that cannot be captured directly; commercial add-on devices or other add-on hardware must be used, including a magnifying lens.

Examples of various add-on attachments and devices for smartphone-based eye imaging are shown in Figure 2.

1) IMAGING OF THE ANTERIOR SEGMENT

The anterior segment of the eye and eye gazes can be captured directly with the smartphone, without any need for additional hardware [28], [30], [32], [38], [39], [43], [51], [56], [57], some of them require super macro mode [46], [58]. To obtain more precise anterior segment data comparable to those in the slit-lamp examination, an attachment mounted

TABLE 2. Anterior segment complete solutions.

Data source	Application (ONLINE/ OFFLINE; Android/ iOS)	Disease	Neural network backbone/ Model description	Use of SP images	First author, year [reference]	Evaluation score*
Face (SP)	Ocular-Diseases App (own) (OFF; An)	Cataract+ other	CNN/ ✓	Tr+Te	Baig, 2023 [27]	●
Eye- red reflex (SP)	EyeScreen (own) (ON; An)	Leucocoria	ResNet-50/ ✓	Tr+Te	Bernard, 2022 [28]	■
Eye (SP)	EE- Explorer (own) (ON; An, iOS)	Ocular emergency	YOLO V3, DenseNet-201, Inception V3/ ✓	Tr+Te	Chen J, 2023 [29]	■
Face (SP)	Appolo Infant Sight (own) (ON; An, iOS)	Visual impairement, amblyopia	EfficientNet-B2, EfficientNet-B4/ ✓	Tr+Te	Chen W, 2023 [30]	◆
Corneal heatmap (SmartKC Topographer) (SP+Topographer)	SmartKC system (own) (OFF; An)	Keratoconus	ResNet-34/ ✓	Tr+Te	Gairola, 2022 [31]	●
Face (SP)	Eyeris (own) (OFF; An)	Heterotropia, strabismus	AlexNet/ ✓	Tr+Te	Gupta H, 2018 [32]	■
Eye (public + SP)	I-Scan (own) (OFF; An)	Cataract	CNN/ ✓	Tr+Te	Neogi, 2024 [33]	■
Face (SP)	Mobile app for data collection and analysis via (IoMT)(own) (ON; An)	Uveitis	U-Net/ ✓	Tr+Te	Perera, 2022 [34]	●
Eye (SP, slit-lamp-full field)	App for inference (own) (OFF; iOS)	Cataract+ other	YOLO V3, YOLO V5, ResNet-101/ ✓	Te	Ueno, 2024 [35]	◆
Eye (SP)	e-Paarvai (own) (ON; An)	Cataract	CNN / ✓	Tr+Te	Vasan, 2023 [36]	■
Face (periocular public dataset)	iCAT (own) (OFF; An)	Cataract	MobileNet V3-Small/ ✓	Tr+Te	Verma, 2022 [37]	■

- "SP"- smartphone, "App"- application, "ON"-online, "OFF"-offline, "An"-Android, "CNN"-Convolutional Neural Network, "Tr"- train, "Te"- test. Model description checkmark- the architecture and basic hyperparameters are described to ensure reproducibility. *Color-coded evaluation score of the article based on Tripod AI: moderate (orange bullet), good (yellow square), excellent (blue diamond).

on a slit-lamp [58] or a digital slit-lamp [45] could be used. An adapter with the light pointed to the left of the pupil was proposed by Quian et al. [55]. An add-on that mimics a real medical device was a low-cost smartphone-based corneal topographer for diagnosing keratoconus, proposed by Gairola et al. [31]. An atypical and creative smartphone add-on, a ring light with a paper-printed grid-like cylinder, was used to screen for dry eye innovatively in contact lens users: if the disease is not detected, a concentric grid of circles is projected onto the eye; otherwise, distorted circles are observed [54].

2) IMAGING OF THE POSTERIOR SEGMENT

To examine the fundus in posterior segment imaging using a smartphone, a fundus adapter with a magnifying lens is used [100]. A 20D condensing lens, as in binocular indirect ophthalmoscopy, is recommended [93]. These adapters, along with smartphone features, enable the capture of images on the go in communities without the need for an examination room or immediate access to electricity and the Internet [9], [10]. In the case of using a smartphone as a fundus camera, all parts can be bought from commercially available sellers [82], [101], [102], [103], constructed and designed (except the lens) from inexpensive and readily available materials (PVC pipes) [82], or printed using three-dimensional printers [68], [87]. More complex prototypes or commercial devices could be attached to the smartphone, such as D-eye [71], [89], [95], [96], Volk-In View [72], Remidio Non-Mydriatic Fundus on Phone [10], [62], [63], [64], [66], PanOptic ophthalmoscope Welch Allyn with iExaminer adapter [78], [84], RetinaScope with 3D printed plastic housing [67], or smartphone-based handheld device Phelcom Eyer [69], [70] (table 6). Among the above-mentioned complex or commercial add-ons, the most widely used fundus-capture mobile device was Remidio Fundus on Phone-Non Mydriatic (Remidio FOP NM) [10], [61], [62], [63], [64], [66]. When using commercially available add-ons, authors usually perform more fundus images– as in [61] posterior pole including disc and macula, nasal and temporal fields and as in [63], [69], and [70] posterior segment centered on macula and one disc-centered image or five sequential images (central, inferior, superior, nasal, temporal) with the possibility to be computationally merged to wide-field montage [67]. To capture an image in a larger field of view, dilation of the pupils (mydriasis) is often used.

The images could be extracted as frames from smartphone-captured video [60], [84], [87], [95], [96]. Using a 3D-printed EyeGo fundus attachment and a Panretinal 2.2 Volk lens on the iPhone, as in [87], allows the authors to extract more data than with single-image capture. The panoptic ophthalmoscope and the iExaminer adapter were mounted on a slit lamp and used as a fixation target to facilitate eye

TABLE 3. Anterior segment- partial solutions.

Data source	Application (ONLINE/ OFFLINE; Android/ iOS)	Disease	Neural network backbone/ Model description	Use of SP images	First author, year [reference]	Evaluation score*
Eye (SP)	TPApp for image acquisition	Pterygium	DeepLab V1, DeepLab V2/ ✓	Tr+Te	Abdani, 2020 [38]	●
Eye (SP)	TPApp for image acquisition	Pterygium	Group-PPM-Net (FC-DenseNet)/ ✓	Tr+Te	Abdani, 2021 [39]	●
Eye (public- dataset)	Android app for inference on public datasets	Cataract	NasNetMobile, Inception V3, VGG19, CNN/ ✓	✗	Charan, 2023 [40]	■
Eye (SP)	TPApp for image acquisition	OSD, dry eye	DenseNet/ ✓	Tr+Te	Chen R, 2021 [41]	●
Eye- photorefraction images (SP)	TPApp for image acquisition	Visual impairment, amblyopia	ResNet-18/ ✓	Tr+Te	Chun, 2020 [42]	●
Face- periocular (DC)	Mobile app for inference (own) (OFF; An)	Heterotropia, strabismus	ResNet-50/ ✓	Tr+Te	de Figueiredo, 2021 [43]	■
Eye (SP)	TPApp for image aquisition	OSD, dry eye	ResNet-50, CNN/ ✓	Tr+Te	Hong, 2021 [44]	●
Eye (SP+slit-lamp-slit beam)	TPApp for image acquisition	Cataract	YOLO V3, ShuffleNet/ ✓	Tr+Te	Hu, 2020 [45]	●
Eye (SP, slit-lamp-full field)	TPApp for image acquisition	Conjunctivitis, keratitis	DenseNet-121, Inception V3, ResNet-50/ ✓	Te	Li Z, 2021 [46]	■
Eye-red reflex (SP+funduscamera)	TPApp for image acquisition	Refractive errors (Myopia)	Inception V3, EfficientNet/ ✓	Tr+Te	Linde, 2023 [47]	■
Eye (SP, slit-lamp-full field)	TPApp for image acquisition	Pterygium	ResNet-101 Faster RCNN, SRU-Net/ ✓	Tr+Te	Liu, 2024 [48]	■
Eye-retro-illumination (slit-lamp- slit beam)	Mobile telehealth app (CC-Guardian) for inference, data collection and analysis via (IoMT) (ON; An, iOS)	Cataract (congenital)	ResNet-101/ ✓	✗	Long, 2020 [49]	■
Everted upper eyelid (DC, public- internet)	Mobile app for inference on public datasets (own) (OFF; An)	Trachoma	CNN (via Google Cloud AutoML)/ ✗	✗	Milad, 2023 [50]	■
Eye- periocular (public-internet)	Mobile app (iConDet) for inference (own)(ON; An)	Conjunctivitis, keratitis	EfficientNet-B4/ ✓	✗	Mukherjee, 2021 [51]	■
Face, red reflex (SP)	TPApp for image acquisition	Visual impairment, amblyopia	CNN/ ✓	Te	Murali, 2020 [52]	●
Eye (public-DC)	Mobile app (Check4Cataract) for inference (own) (OFF; An)	Cataract	MobileNet V2/ ✓	✗	Nair, 2023 [53]	●
Eye (SP+ring light+ grid-like cylinder)	TPApp for image acquisition	OSD, dry eye	ResNet-50/ ✓	Tr+Te	Okazaki, 2023 [54]	●
Eye (SP+slit-lamp-full field)	TPApp for image acquisition	Refractive errors (Myopia- ACD)	ResNet-34/ ✓	Tr+Te	Qian, 2022 [55]	●
Eye (SP)	TPApp for image acquisition	Cataract	AlexNet, GoogLeNet, VGG16, ResNet-50, Inception V3/ ✓	Tr+Te	Ramlan, 2023 [56]	●
Face (SP)	TPApp for video recording	Periorbital measurements	U-Net with ResNet-50/ ✓	Te	Van Brummen, 2021 [57]	■
Eye (SP and DC +slit-lamp- full field)	TPApp for image acquisition	Conjunctivitis, keratitis	Inception V3, ResNet-50, DenseNet-121/ ✓	Te	Wang, 2021 [58]	●
Ocular surface (public-internet, including SP)	TPApp for image acquisition	Conjunctival melanoma	GoogLeNet, Inception V3, NasNet, ResNet-50, MobileNet V2, CycleGAN, PGGAN/ ✓	Te	Yoo, 2021 [59]	●
Eye-lateral segment (SP)	TPApp for video recording	Keratoconus	VGGNet-16/ ✓	Tr+Te	Zaki, 2021 [60]	●

- "SP"- smartphone, "ON"-online, "OFF"-offline, "An"-Android, "NS"-not specified, "DC"-digital camera, "App"- application, "ACD"-Anterior chamber depth, "CNN"- Convolutional Neural Network, "OSD"- Ocular surface disease, "Tr"- train, "Te"- test,"TPApp"-Third party app. Model description checkmark- the architecture and basic hyperparameters are described to ensure reproducibility. *Color-coded evaluation score of the article based on Tripod AI: moderate (orange bullet), good (yellow square), excellent (blue diamond).

TABLE 4. Posterior segment- complete solutions.

Data source	Application (ONLINE/ OFFLINE; Android/ iOS/web)	Disease	Neural Network backbone/ Model description	Use of SP images	First author, year [reference]	Evaluation score*
"Remidio NM-FOP"+SP, public-dataset, FC	App for inference (Medios) (OFF; iOS)	DR	Inception V3, MobileNet/ ✓	Tr+Te	Natarajan, 2019 [61]	◆
					Sosale, 2020 [10]	■
					Jain, 2021 [62]	◆
					Kemp, 2023 [63]	■
"Remidio NM-FOP"+SP, FC	App for inference (Medios AI-Glaucoma) (OFF; iOS)	Glaucoma	Feature Pyramid Network with ResNet-50/ ✓	Tr+Te	Rao, 2023 [64]	■
					Shroff, 2023 [65]	■
"Remidio NM-FOP"+SP, FC	Cloud software for inference (EyeArt) (ON;iOS)	DR	cloud-based/ ✗	Te	Rajalakshmi, 2018 [66]	●
"RetinaScope"+SP	Cloud software for inference(EyeArt) (ON; iOS)	DR	cloud-based/ ✗	Te	Kim T, 2021 [67]	●
3D camera module+SP, public- dataset	Mobile app for inference(own) (ON; An)	DR	Exception V3/ ✓	Te	Kim W, 2022 [68]	■
"Eyer"+SP	Cloud software for infer- ence (EyerCloud)(ON; An)	DR	cloud-based (Xception)/ ✓	Tr+Te	Malerbi, 2022 [69]	■
"Eyer"+SP, public- dataset	Cloud software for infer- ence (EyerCloud+EyerMaps) (ON; An)	DR	cloud-based (Xception)/ ✓	Tr+Te	Penha, 2023 [70]	■
"D-Eye"+SP, public- dataset	Mobile app for inference(own) (ON; An, iOS)	DR	Xception/ ✓	Te	Wei, 2019 [71]	■
"Volk-InView"+SP	Mobile app for inference (own) (OFF; An)	DR	NasNet-Mobile as FE+MLP/ ✓	Tr+ Te	Elloumi, 2022 [72]	■
Portable optical device+SP, own FC, public-dataset	Mobile app (Diavision) for inference (own) (ON; web)	DR	CNN as FE+ML/ ✓	Tr+Te	Alves, 2020 [73]	■
microscopic lens+SP	Android app for inference on public datasets (OFF; An)	Cataract (+other)	MLP/ ✓	Te	Bourouis, 2014 [74]	●

Data are sorted according to the capturing device or smartphone attachment listed in data source column. "SP"- smartphone, "FC"- captured using fundus-camera, "App"- application, "ON"-online, "OFF"-offline, "An"-Android, "DR"-diabetic retinopathy, "ROP"- retinopathy of prematurity, "FE"- feature extractor, "ML"-machine learning, "MLP"- Multilayer Perceptrone, "Tr"- train, "Te"- test. Model description checkmark- the architecture and basic hyperparameters are described to ensure reproducibility. *Color-coded evaluation score of the article based on Tripod AI: moderate (orange bullet), good (yellow square), excellent (blue diamond).

alignment during video recording in [84]. After capturing the video using the D-eye device, the best frame was chosen manually [89], [95]. The best five images were manually selected in [84] and [78].

In the following subsections, we summarize the capture of eye images under different gazes, distances, and lighting conditions. The last subsection is devoted to red reflex, mydriasis, and pupil extraction. It is also necessary to consider the type of camera used. Some systems utilize both front and rear cameras, with the help of another person in the latter case [32].

3) GAZES AND ANGLES

More relevant data could be extracted when captured from different gazes [28], [43], similar to the standard ophthalmological examination. The upward, right, and left gazes were added to the central gaze to detect leukocoria [28], nine direction gazes in the strabismus classification application [43]. Lateral segment images captured from the side view could help diagnose keratokonus [60]. One application captures images at a specified angle, using data from the accelerometer and gyroscope sensors embedded in the smartphone [32].

4) CAPTURING DISTANCE

Capturing direct images from three distances was proposed in [52] to obtain adequate images under different light conditions. To assess the correct, standardized photo shooting distance, software that detects eyes and frames them in real-time could be helpful [28]. A 15-centimeter distance

TABLE 5. Posterior segment- partial solutions.

Data source	Application (ONLINE/ OFFLINE; Android/ iOS/web)	Disease	Neural network backbone/ Model description	Use of SP images	First author, year [reference]	Evaluation score*
public- dataset	Mobile app for inference (own)(OFF; An)	DR (DME)	DenseNet-121/ ✓	✗	Al-Absi, 2023 [75]	■
public- dataset	Mobile app for inference (own)(OFF; An)	Pathological myopia	MobileNet V3/ ✓	✗	Ali, 2022 [76]	◆
public- dataset	Mobile app (RetinoCare) for inference (own) (ON & OFF; An, web)	DR	ResNet-50(web), MobileNet (app)/ ✓	✗	Bidari, 2021 [77]	◆
"Welch Allyn Panoptic ophthalmoscope"+ SP	iExaminer third party app for image acquisition	Glaucoma	DenseNet, MobileNet, Inception V3, InceptionResNet, ResNet-50v2, ResNet-101, Xception/ ✓	Tr+Te	Braganca, 2022 [78]	■
public- dataset	Mobile app for inference (own) (OFF; An)	Cataract (+other)	MobileNet V2/ ✓	✗	Elloumi, 2021 [79]	◆
public- dataset	Mobile app (Diabetic Vision) for inference (own) (OFF; An)	DR	Inception V3/ ✗	✗	Ghouali, 2022 [80]	◆
public-dataset+ FC	Mobile app (Yanbao) for inference (own) (ON; iOS)	Glaucoma	U-net/ ✓	✗	Guo, 2018 [81]	■
DIY camera+SP	TPApp for image acquisition or video recording	DR	CNN/ ✓	Te	Gupta S, 2022 [82]	◆
public- dataset	Mobile app for inference (own) (OFF; An)	DR	Inception/ ✓	✗	Hagos, 2019 [83]	◆
"Welch Allyn Panoptic ophthalmoscope"+SP	iExaminer TPApp for image acquisition	Retinal vessels analysis	U-net/ ✓	Te	Hu, 2020 [84]	■
public- dataset	Mobile app for inference (own) (OFF; An)	Cataract (+other)	MobileNet V2/ ✓	✗	Intaraprasit, 2023 [85]	◆
public- dataset	Mobile app (Deep Retina) for inference (own) (ON; iOS)	DR	DCNN/ ✓	✗	Li YH, 2019 [86]	◆
"EyeGo" +SP(attached to slit-lamp)	TPApp for video recording	DR	DenseNet-201/ ✓	Te	Ludwig, 2020 [87]	◆
own FC	Mobile app for inference (own)(ON; An)	ROP	ResNet-101/ ✓	✗	Luo, 2022 [88]	◆
"D-Eye"+SP	TPApp for video recording	Glaucoma	SR-GAN + CNN/ ✓	Tr+Te	Maddala, 2022 [89]	◆
public- dataset	Mobile app for inference (own) (OFF; An, iOS)	DR	Inception V3/ ✓	✗	Majumder, 2020 [90]	◆
public-dataset	Mobile app for inference (own) (OFF; An)	Glaucoma	U-net, MobileNet V2, VGG16, VGG19, Inception V3, ResNet-50/ ✓	✗	Martins, 2020 [91]	◆
public- dataset	Mobile app for inference (own) (OFF; An)	DR	EfficientNet-B0/ ✓	✗	Matthew, 2023 [92]	◆
SP+20D lens	Mobile app for image acquisition	ROP	U-Net/ ✓	Tr+Te	Mutua, 2023 [93]	◆
public- dataset	Mobile app for inference (own) (OFF; An)	DR	MobileNet, VGG-16, Inception V3, ResNet-50/ ✓	✗	Nage, 2022 [94]	◆
"D-Eye"+SP	TPApp for video recording	Glaucoma	ResNet-34/ ✓	Te	Nakahara, 2022 [95]	■
"D-Eye"+SP	TPApp for video recording	Glaucoma	Inception ResNet V2, Inception V3, U-Net/ ✓	Te	Neto, 2022 [96]	■
public- dataset	Mobile app (FundusNet) for inference (own) (ON; web)	DR	Xception, VGG-16, ResNet-152, MobileNet V2, EfficientNet-B7/ ✓	✗	Shrimali, 2023 [97]	◆
own FC, Volk 28D lens+SP	TPApp for image acquisition	ROP	Inception V1/ ✓	Tr+Te	Subrammaniam, 2022 [98]	◆
public- dataset	Mobile app for inference (own) (OFF; An)	DR	MobileNet/ ✓	✗	Suriyal, 2018 [99]	◆

- "SP"- smartphone, "FC"- captured by funduscamera, "App"- application, "ON"-online, "OFF"- offline, "An"-Android, "CNN"- Convolutional Neural Network, "DME"- diabetic macular edema, "DR"- diabetic retinopathy, "ROP"- retinopathy of prematurity, "Tr"- train, "Te"- test, "TPApp"-Third party app. Model description checkmark- the architecture and basic hyperparameters are described to ensure reproducibility.
*Color-coded evaluation score of the article based on Tripod AI: moderate (orange bullet), good (yellow square), excellent (blue diamond).

FIGURE 2. Various smartphone add-on attachments and devices used in reviewed articles for smartphone imaging in ophthalmology and their price estimates in US dollars (USD). The red background of the price represents high-end solutions, yellow background mid-range solutions, and finally blue represents low-cost solutions.

Attachments and devices used in first row (from left to right): Remidio NM-FOP: [10], [61]– [66] , Eyer [69], [70], RetinaScope [67], Volk-InView [72], D-Eye [71], [89], [95], [96], Smartphone with microscopic lens [74]; in second row (from left to right): portable optical device [73], Panoptic ophthalmocope Welch-Allyn [78], [84], Do it yourself funduscamera [82], SmartKC Topographer [31], Ring light and grid-like cylinder [54], Smartphone adapter on slit-lamp [55].

TABLE 6. Complex prototypes or commercially available devices to examine fundus with smartphone in reviewed articles.

Product name	Company	Smartphone	FOV	AI
D-EYE	-	iPhone 5	5-8°/ 20°*	-
Remidio FOP NM	Remidio	iPhone SE	40°*	Medios
iNview	Volk Optical	iPhone 5s, 6, 6s, SE	50°/80°*	-
RetinaScope	-	iPhone 5s	50°*,**	-
PanOptic Ophthalmoscope	Welch Allyn	-	20°	-
Eyer	Phelcom	Samsung Galaxy S10	45°*,**	EyerMaps
PaxosScope (prev. EyeGo)	DigiSight	iPhone 5S	55°*	-

- "FOV"-Field of view, "AI"- Artificial Intelligence system included, *-non-mydriatic mode also available, **- system includes software to montage the different-angle images into one stereoscopic fundus image, increasing the field of view

with the lower eyelid pulled down was ideal for the work to visualize the bulbar and tarsal conjunctiva with a tear film to detect dry eye disease [44]. A distance of less than 20 cm was reported in [41] to capture the ocular surface and detect ocular surface disease (OSD).

5) LIGHT CONDITIONS

Capturing images under different/lower light conditions should also be considered, for example, in dim or dark conditions [67], [84]. The dark room was used to capture eccentric photorefraction images at a distance of one meter [42]. A smartphone flashlight can be refracted, magnified, and reflected from the retina, creating a crescent-shaped reflection in the pupil [42]. Infrared and color-red reflexes were captured in [47] to observe crescents in the pupil in automatic refractive error estimation. Screening for media opacities and leukocoria was performed in dark and ambient conditions to capture red reflex [28]. In [52], the authors measured parameters such as the position of the red reflex, the radius of the undilated pupil, the hue of the iris region, the red reflex and crescent width from dark-lit images, and eyelid contour, corneal light reflex, and the center of the iris from images of ambient light. To reduce accommodation and pupil constriction, infrared images were captured in a dark room, as with the Nun infrared camera attached to a smartphone [47]. Diffuse light and side-focused illumination from a slit light to the nuclear region of the lens, similar to standard ophthalmoscopic examination, were proposed by [45] for cataract screening using a smartphone-attached slit lamp. The macro mode of the rear cameras allows for automatic focus at very short distances with high resolution, as in [46], and [58].

6) RED REFLEX, MYDRIASIS AND PUPIL EXTRACTION

Red reflex images are used to help diagnose cataract, leucocoria, amblyopia, and refractive errors (with the use of photorefraction images). Capturing the eye, including the red reflex, is very challenging. As it was difficult to capture faces without ''red eyes'' in the past, it is now complicated to capture eyes with red reflex with current technologies. In current smartphones, various methods are implemented to avoid red reflex, as an often unintended phenomenon, i.e., a pre-flash of bursting on the object before capturing the image, or several built-in post-processing algorithms. Bernard et al. [28] captured naturally dilated eyes with a red reflex in a dark environment, and by turning off pre-flash settings. The same approach, removal of the pre-flash, was proposed by Murali

et al. [52]. Both solutions lack reproducible technical details on how to modify the pre-flash settings. Linde et al. [47] captured red reflex images using an infrared fundus camera.

When capturing the fundus, most works use pupil dilation (mydriasis) [62], [67], [69], [70], [93]. The examination of the fundus through a dilated pupil is easier and more accurate, and is also necessary when examining some other ocular structures, such as the lens. It reduces the pupil-induced artefacts, helping us to obtain images of higher quality. It widens the field of view, allowing us to detect pathologies in the retinal periphery. In addition, it is helpful in non-cooperative patients, especially in pediatric ophthalmology, to examine the patient faster. Capturing images without mydriasis avoids the risk of angle closure in previously unexamined patients with a narrow anterior chamber angle. The field of view is reduced, but could still be sufficient to screen some of the ophthalmologic pathologies. The advantage is the ability to screen ''on the go'' without any medical assessment. Capturing the fundus without dilation of the pupil could be handled when capturing images in the dark using an infrared light source, which could be found as an additional feature in [10], as in the Remidio NM-FOP device.

In some research, there is a need for pupil extraction, regardless of whether it contains the red reflex. Haar cascade [104] was used to detect pupils and bound them to the circle in [32]. Dlib face landmarks detection extracts the eyes using Histogram of Oriented Gradients features along with a linear classifier to detect the pupil from whole-face images [37].

C. IMAGE DATASETS USED IN SMARTPHONE DEEP LEARNING APPLICATIONS, PREPROCESSING AND AUGMENTATION TECHNIQUES

Authors of analyzed papers worked with own datasets, some of which were captured by the smartphone [28], [32], [43], [52], [73], [81], some with a standard slit lamp or fundus camera [73], or with publicly available datasets [10], [71], [73], [79], [81], [87], [90], [91] (Table 7). Datasets could also be collected from publicly accessible images from the web based on specific keywords [59]. There are almost no public ophthalmologic datasets captured by smartphones available, except for two: – the first, the Brazil glaucoma dataset with 2000 images, focused on the optic disc and glaucoma diagnosis [78], and the second, the Cataract Mobile Periocular Database (CMPD) [105] with 2380 direct smartphone images before and after cataract surgery.

1) DATA COLLECTION

When collecting the data, it is useful to collect the demographics. It is unclear how the described deep learning models performed across different demographics; nevertheless, 10 of 34 anterior segment solutions listed the age and gender of participants, three more listed just the age, and the rest of the articles did not mention the age and gender. From the posterior segment solutions, 12 of 40 articles mentioned age and gender. Some of the articles focus on child patients (i.e., retinopathy of prematurity, amblyopia detection). In addition to the average statistics, no performance analysis was performed according to the age or gender.

When using their own dataset, in most articles, the participants were tested in one country, except in two works where the participants were tested in two countries [47], [50]. On the other hand, a multi-institutional collection of participants was present in more works, which confirmed the robustness of the studies. More than 10 institutions or centers were present in four studies [35], [49], [61], [62], and 2 to 9 institutions in 11 studies. Cross-platform or cross-device validation may contribute to the availability of the solution. If provided, most solutions use Android smartphones, seven solutions use both iPhone and Android [29], [30], [48], and two solutions are marked cross-platform [34], [43]. In complete posterior solutions are mainly used iPhones, but this could be explained because almost half of the solutions are captured using the Remidio FOP camera. Few of the reviewed studies validated models on independent external datasets, and if this was present, it was mostly in posterior partial solutions, when using a public dataset and testing or training on a smaller private smartphone dataset.

To obtain a standardized and homogeneous dataset, it is common practice to present images acquired under constrained conditions. In anterior segment solutions, almost half works (16 of 34) described some reproducible constrained conditions, which differ from each other. In posterior segment solutions, especially in the complete subgroup, the majority of solutions use commercially available devices, which usually have recommended user instructions and settings for capturing the image in constrained conditions. Some solutions implemented an image-quality check after capturing to focus on image clarity, integrity, and illumination [29], which could be helpful when capturing on different devices or platforms (i.e., iPhone with Android). Besides that, there is no standardized test that could be used to judge the quality of anterior and posterior eye images across smartphone devices. Implementing such a test could be valuable as a future research goal to compare images or even whole datasets obtained from different devices.

Patient consent is absolutely essential in any form of medical imaging, ensuring that individuals control how their personal health information and images are used, particularly for research or sharing outside direct clinical care. Although most authors acknowledge that they have obtained patient consent for their study, they typically do not discuss the potential implications arising from such consent, particularly with regard to data handling and usage permissions. The consent scope must be clearly defined to prevent misunderstandings or misuse of sensitive medical information post-consent. Furthermore, even after receiving explicit consent, ensuring privacy often involves deidentification - the process of removing personal identifiers (like name, date of birth) from data. However, under regulations like General Data Protection Regulation (GDPR), which emphasize strict data minimization and purpose limitation before any processing,

TABLE 7. Publicly available datasets used in reviewed articles.

Database Name	Source	Disease	No of Images	Open Access	Upon request
APTOS 2019 Blindness Detection [106]	F	DR	3,662	✓	✗
Cataract mobile periocular database(CMPD) [105]*	D	Cataract	2,380	✓	✗
Dataset Brazil Glaucoma (BrG) [78]*	F	Glaucoma	2,000	✓	✗
Diabetic retinopathy detection (EyePACS), Kaggle [107]	F	DR	88,702	✓	✗
DiaretDB0 [108]	F	DR	130	✓	✗
Drishti-GS [109]	F	Glaucoma	101	✓	✗
High resolution fundus (HRF) [110]	F	DR, Glaucoma	45	✓	✗
IDRiD [111]	F	DR	413	✓	✗
Kaggle cataract dataset [112]	F	Cataract, glaucoma, other-posterior	601	✓	✗
Messidor [113]	F	DR	1,200	✓	✗
ODiR [114]	F	Other- posterior	6,392	✓	✗
ORIGA light [115]	F	Glaucoma	650	✓	✗
PALM: Pathologic myopia challenge [116]	F	Pathologic myopia	1,200	✗	✓
REFUGE (iChallenge-GON) [117]	F	Glaucoma	1,200	✗	✓
RIGA [118]	F	Glaucoma	460	✓	✗
RIM-ONE r3 [119]	F	Glaucoma	318	✓	✗
Sclera Blood Vessels, Periocular and Iris (SBVPI) [120]	D	Uveitis	1,858	✗	✓
STARE [121]	F	Other- posterior	402	✓	✗

- "F"-fundus photography, "D"- direct photography without any attachment, "DR"-diabetic retinopathy, *-smartphone captured

including storage or sharing for research, the complete anonymization is not always guaranteed by simple deidentification; residual risks may still exist depending on the techniques used (e.g., pseudonymization might allow re-identification under certain circumstances). This omission highlights the need for research centers to proactively consider possible uses (including future studies, secondary analysis, teaching materials) when obtaining consent, ensuring that patients are fully informed and agree specifically to each intended application. Failure to do so can lead to ethical breaches even after initial permission is granted.

2) ANTERIOR SEGMENT DATASETS

The described anterior segment images are direct images captured without additional attachments (in 25 of 74 reviewed articles) (Figure 3, first and second rows) and images captured with a slit lamp (7 of 74) (Figure 3, third row). Additional specific components mentioned only in two articles were a smartphone-based corneal topographer [31] to capture corneal heat maps for the screening of keratoconus and a grid-shaped cylinder with ring light to diagnose dry eye [54].

After the analysis of the reviewed articles, we can confirm that it is possible to capture images of the anterior segment of the eye of sufficient quality for diagnostic purposes with a smartphone without any attachment. Images acquired using a smartphone-attached slit lamp could also be of sufficient quality, focusing on more superficial structures with full spread of light or on deeper structures using the slit beam from the slit-lamp. This could be considered according to the target eye structure or disease.

3) POSTERIOR SEGMENT DATASETS

When analyzing smartphone fundus images, the quality differs significantly. It also depends on whether a simple 3D printed fundus attachment is used or a commercially available device with built-in preprocessing and image quality control assessment. Some applications are trained using fundus images captured with a standard fundus camera and tested on smartphone-captured images. When captured in low quality, the results could be unreliable. Therefore, various preprocessing techniques are used; some authors prefer to capture more images or preferentially extract images from smartphone-captured video [78], [84]. As public fundus image datasets, mostly EyePacs [112] and Asia Pacific Tele-Ophthalmology Society (APTOS) [106] datasets were used. These datasets could be downloaded from the Kaggle data science community. The largest dataset from reviewed articles was used by [87], the authors combined EyePacs and APTOS datasets with their own dataset extracted from smartphone shot videos.

4) IMAGE PREPROCESSING

As a pre-processing, CLAHE [122] was used in several works [79], [82], [84], [91], [93], [98], channel-wise color normalization [53], and conversion to a green channel due to higher contrast [82], [98]. Segmentation of the image based on color spaces and masking was proposed by [51], expanding the 3 to 4 color channels in [55]. The mask of the fundus region could be assumed by using the Hough transform [98]. The authors in [89] and [99] used noise removal filters. Multiscale retinex with preservation of chromaticity was used to enhance image quality in [56]. In addition, blood vessel extraction was used [81], [84], overall with median filtering and morphological operations [81]. Gamma correction could be applied to better visualize endpoints of tiny vessels [93]. The triplet-based method and the watershed transform were used to detect the optic disc in [82]. The authors in [45] use the Tenengard algorithm, a gradient-based image definition evaluation function using the Sobel operator, to select the output image for further analysis. To detect the eye region on the video or image, the authors in [27], and [32] used the Haar cascade proposed by Viola and Jones [104].

In the reviewed articles, it is not explicitly mentioned how the authors deal with the reflections of bright lights when capturing images with a smartphone. These reflections could

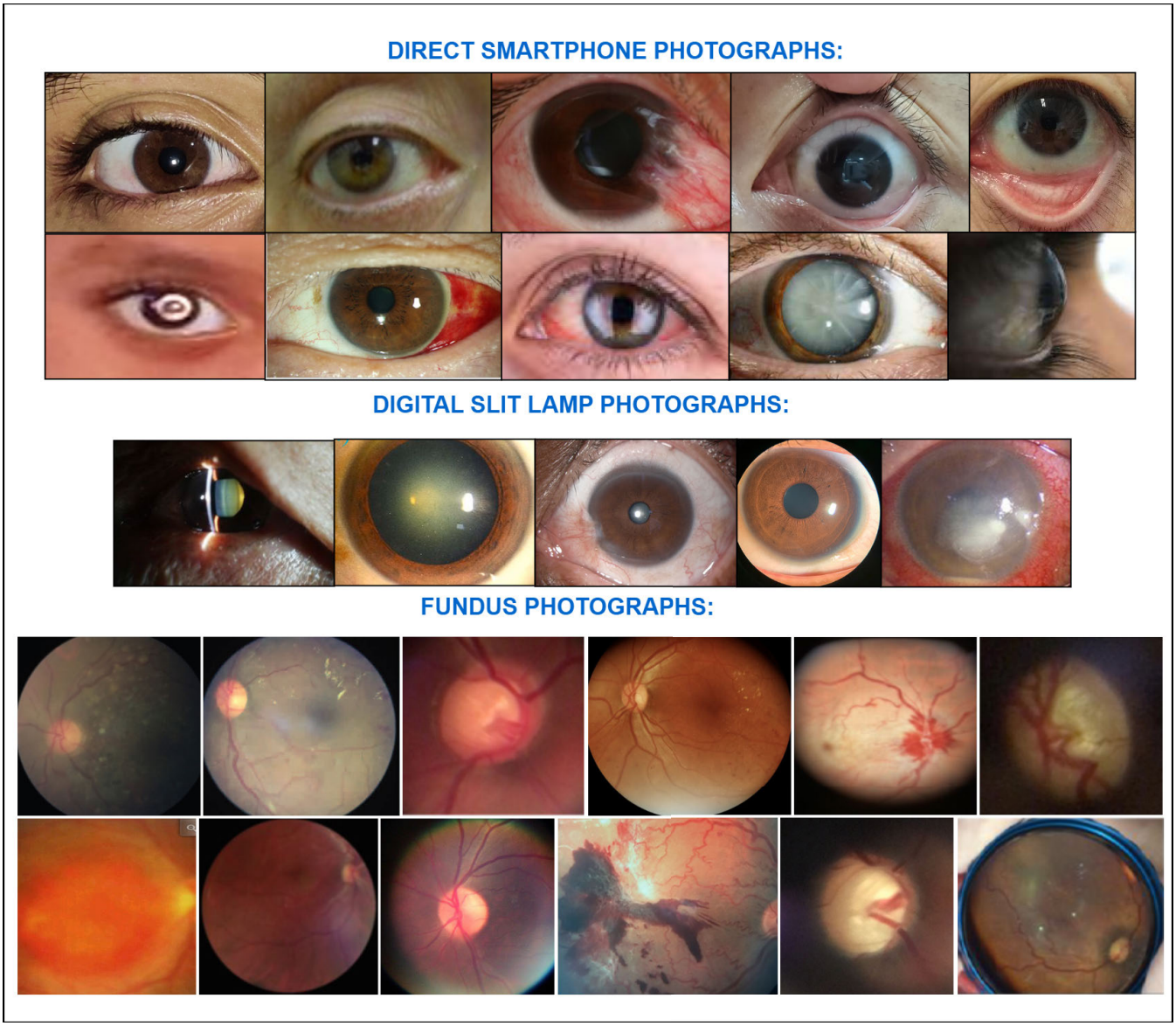

FIGURE 3. Examples of image datasets - captured directly with smartphone (first two rows), captured using smartphone portable slit-lamps or digital slit-lamps (third row), and fundus images captured using various smartphone attachments or commercial devices connected to smartphone (fourth and fifth rows).

First row (from left to right): [27], [43], [38], [41], [44], second row (from left to right): [28], [29], [51], [53], [60], third row (from left to right): [45], [58], [48], [55], [35], fourth row (from left to right): [62], [61], [78], [70], [71], [96], fifth row (from left to right): [74], [72], [84], [87], [95], [98].

alter the image and make further diagnosis challenging; an image quality check could prevent the use of such undesired images.

5) IMAGE AUGMENTATIONS

Usually, various augmentation techniques are used to enlarge and balance the dataset before deep learning training. Augmentation includes various approaches: rotations [55], flipping and zooming [10], [28], [43], [51], [55], [61], [87], perspective distortion [43], changing aspects of color [28], [43], [53], [91], and Gaussian, average, median, or motion blurring [30], [52], [91].

To augment the dataset, more images of both eyes could be used: complete eye or anterior segment of the eye, different gazes or angles [28], [43]. Quite a lot of images could be extracted by capturing videos [30], [87]. Augmentations could be saved on the drive or generated in real-time to save disk space and train using different images in each batch [91]. In the paper [59], a novel trend was applied in which GAN models generated synthetic images of conjunctival lesions to augment the dataset.

D. DEEP LEARNING MODELS

The reviewed articles used various neural networks (NNs), with a strong focus on deep learning (DL) models. These models were used primarily for classification tasks, dividing patients into healthy and unhealthy, or referable and non-referable, and in some applications even into multiple classes

according to the stage of the disease. Other possibilities of use include segmentation, object detection, regression, and image generation. In particular, several studies have included DL methods for image quality monitoring [30], [61]. Furthermore, Maddala et al. [89] implemented image quality enhancement through super-resolution generative adversarial networks (SRGAN) to improve datasets for glaucoma classification. Moreover, synthetic image generation using GAN models was adopted by Yoo et al. [59] to augment datasets. In some cases, the DL models were limited to feature extraction in conjunction with other classifiers [72], [73], [79], [83], while another study used DL for prediction purposes [55].

In general, used DL models differ regarding performance, efficiency, or suitability for mobile deployment. MobileNet, with an extremely low parameter count and latency, was designed for mobile deployment. Together with ShuffleNet, they are very efficient for smartphone use, offering fast inference, low memory use, and moderate accuracy [123], [124], although their accuracy may decline further when working with small datasets. This can be addressed when tuned to domain-specific tasks. EfficientNet models offer higher accuracy, making them one of the most efficient modern architectures, but the size of the models differs according to the used version (5 to 50 MB) [125]. Like some larger versions of the EfficientNet model, larger models (i.e., ResNet, Unet, DenseNet, Inception, XCeption, NasNet) provide excellent accuracy, but have a slower inference speed and often require pruning or quantization to run efficiently on mobile devices [126]. Cloud deployment presents another viable option, which requires an Internet connection and could raise latency and privacy concerns [127]. U-net is usually the most common and accurate model used for segmentation, especially for medical images, but requires a lightweight variant with fewer parameters and optimization when deployed on mobile devices [128]. YOLO (You Only Look Once) models are fast and accurate and are typically used for object detection, but like U-net, they often require some modifications when used in low-resource environments [129].

The analysis revealed 11 complete solutions for the anterior segment, with nine relying on DL for classification. Among them, one study used DL for object detection [29], one study employed DL for segmentation [34], and one study utilized DL for feature extraction [30] (Table 2).

For partial anterior segment solutions, 23 studies were analyzed. Among them, 15 used DL exclusively for classification, two employed DL for segmentation [38], [39], one for regression [55], and 2 for combined classification and detection [45], and detection with segmentation [48] (Table 3).

In the anterior segment, ResNet-based models were predominantly used for classification tasks, followed by Inception models (Figure 4). YOLO detectors were utilized as object detectors, while U-net-based models and ResNet models were used for segmentation and regression, respectively.

A summary of 15 complete posterior segment solutions revealed that 11 studies used DL for classification, two used it for segmentation, and another two combined classification and feature extraction (Table 4).

Among the 25 partial posterior segment solutions, 17 used DL for classification, 2 for segmentation [81], [84], 2 for feature extraction [79], [83], one for image generation and classification [89], and another two for combined classification and segmentation [91], [96] (Table 5).

Overall, posterior segment studies relied primarily on MobileNet-based and Inception models for classification, followed by ResNet-based models. U-net models were predominantly used for segmentation tasks, such as optic disc and cup segmentation or retinal blood vessels detection. These findings were influenced by four articles that used a shared solution (Remidio FN-Top with the MEDIOS system) [10], [61], [62], [63] (Figure 5).

The primary architectures utilized for the anterior and posterior segment solutions are models based on ResNet and Inception, with the difference in the use of MobileNet-based architectures, which also dominate in posterior segment solutions. Because most of the solutions reviewed are partial, this discrepancy might be caused by a different proportion of solutions with applications for inference. If a solution contains an application for inference, the model is usually implemented in a smartphone. The prevalence of inference applications is much higher in partial posterior segment solutions compared to anterior segment partial solutions (16 of 25 solutions vs. 6 of 23 solutions). Thus, we could expect more use of MobileNet-based architectures, which were primarily designed for mobile deployment. On the other hand, the prevalence of image acquisition or video recording applications dominates in partial anterior segment solutions (16 of the 23), making it less essential to use a lightweight model.

We compared all solutions in which the accuracy metric was listed, solving binary or multiclass classification problems. The highest average accuracy in binary problems was achieved by NasNet mobile, U-net, and VGG (descendingly) (Fig.5, top left image). If we analyze specificity versus sensitivity, the highest classification performance can be observed at VGG, the Ensemble model, and Inception. Variable performance was observed in MobileNet, ResNet, and Cloud solutions. Xception and custom CNN gained higher sensitivity, but lower specificity (Fig.5, top right image).

In multiclass solutions, MobileNet, ShuffleNet+SVM, and custom CNN achieved the highest average accuracy. We observed that in multiclass solutions, the use of a DL model is not the case, so variable-used models are repeated (Fig.5, bottom left image). Due to the availability of enough solutions to classify diabetic retinopathy into severity stages, we have compared the DL models according to overall accuracy. Almost all solutions gained similar accuracies, except for one Inception and one custom CNN model with the highest values (Fig. 5, bottom right image).

To avoid time-consuming and data-demanding training from scratch, most studies employed transfer learning by

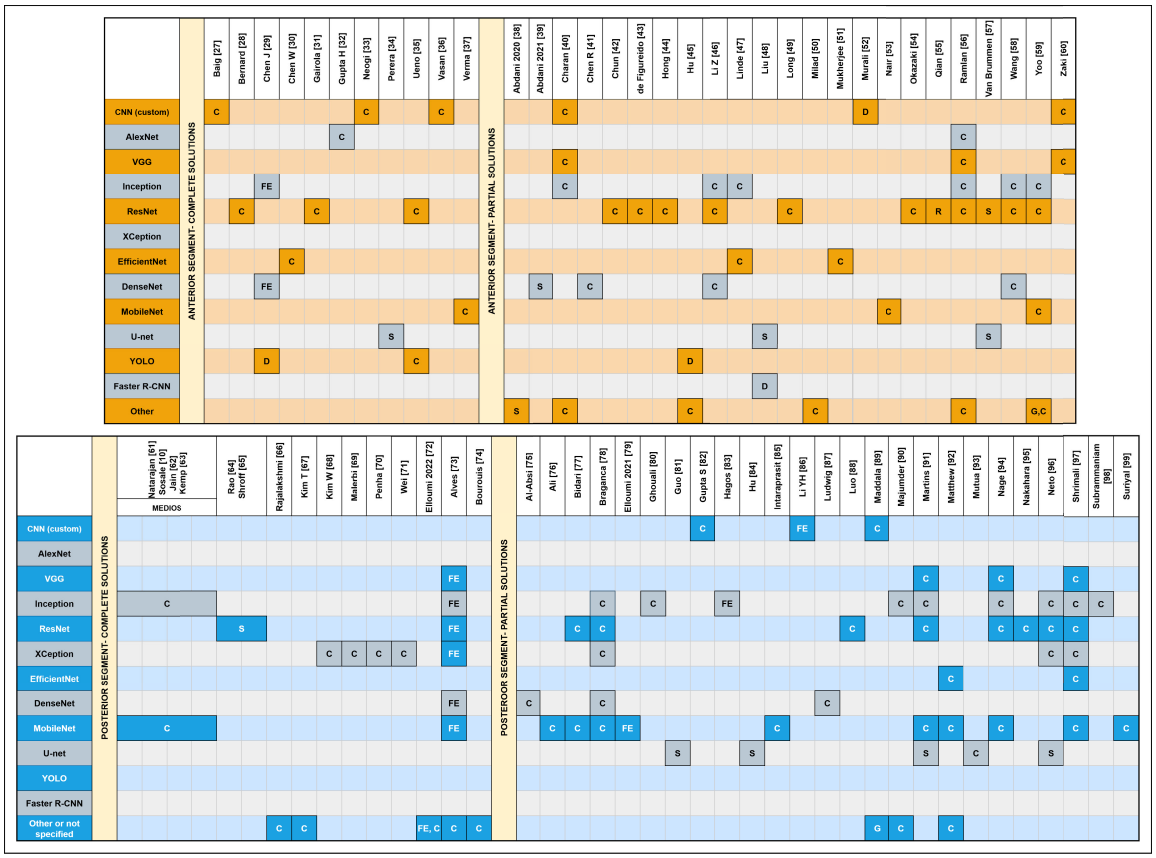

FIGURE 4. Deep learning models used in anterior (first table) and posterior segment (second table) solutions in reviewed articles. "C"- classification, "D"- object detection, "S"- segmentation, "FE"- feature extraction, "R"- regression, "G"- image generation.

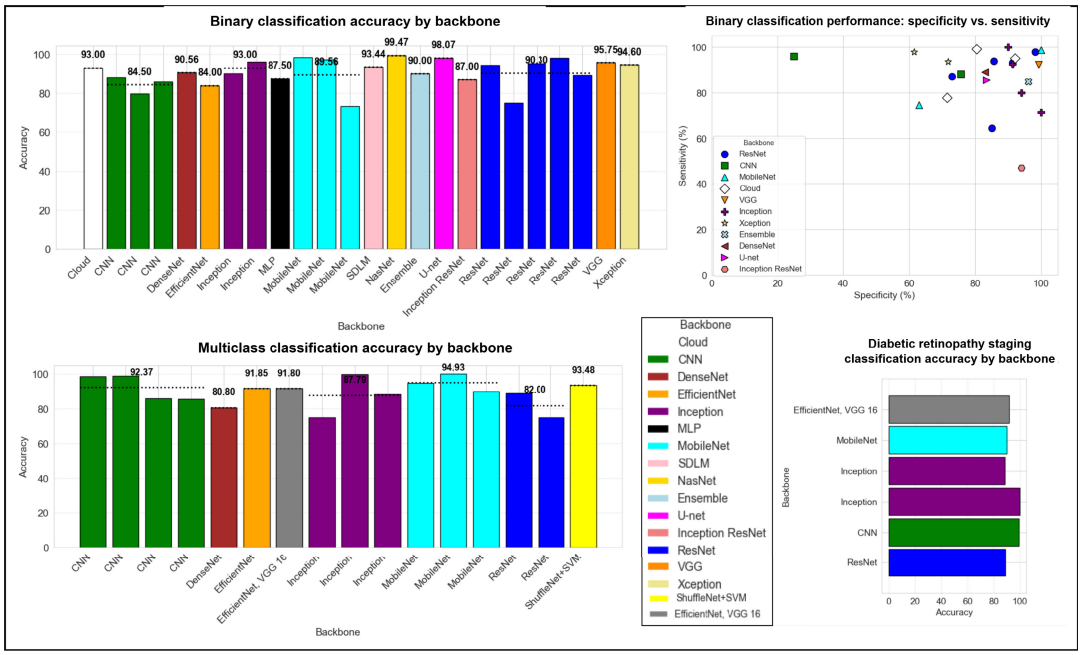

FIGURE 5. Graphs of binary and multiclass accuracy, binary classification performance, and diabetic retinopathy staging classification accuracy.

pre-training DNNs on the ImageNet database [130] before fine-tuning them on target datasets. Detailed information regarding the specific DL models used, including their evaluation metrics (e.g., accuracy, sensitivity, specificity, and AUC), is provided in Appendix Tables 8-11.

E. TECHNICAL SOLUTIONS FOR DEPLOYING DEEP LEARNING MODELS

The analysed smartphone deep learning applications are diverse and differ in implementations, programming languages used, computing resources used, and other technical specifications. However, we can divide them into online and offline solutions, depending on whether they need an internet connection to function correctly or not.

1) OFFLINE SOLUTIONS

Offline solutions do not require access to the Internet and can be used for screening purposes in remote areas where a stable Internet connection is not currently available. On the other hand, these applications are usually hardware dependent, which can lead to specific limitations and increased complexity of the overall solution. In this approach, the deep learning model is deployed directly in a standalone native mobile application by default, which allows for local analysis of input images captured by the device's camera or stored in the phone's memory (Figure 6). In general, the speed of evaluation by a deep neural network varies based on the specific mobile device and its computing capabilities. To speed up calculations, hardware acceleration is often used, which enables the processing of computationally intensive operations by the graphics processing unit (GPU) or application-specific integrated circuit (ASIC). This leads to offloading a general-purpose central processing unit (CPU) and speeding up the evaluation process even on mobile platforms, as recently shown by Martins, Cardoso, and Soares [91]. Since a large number of smartphones have embedded GPUs, utilizing hardware acceleration is usually preferred when available [55].

2) ONLINE SOLUTIONS

The second type is represented by solutions that require temporary access to the Internet in the form of a native mobile application, or during the entire process of using the mobile platform through a web application (Figure 6). Online solutions are not hardware dependent on a specific mobile device and can have an additional feature: they could contain a doctor's opinion module in a telemedicine, meaning an external expert consultation [81], [131]. The main reason for the need for active access to the Internet is the connection to the cloud server for computational offloading. The online cloud server usually has higher computing capabilities than the user's mobile device, which enables the acceleration of sample evaluation and the use of more complex and computationally demanding deep neural networks, which could not be directly deployed on a mobile platform. In addition, the computing server can also fully utilize the possibilities of hardware acceleration, in general, by using GPUs. In terms of implementation, several solutions rely on sending a sample from the mobile device to a cloud computing server, where it is analyzed and the result is sent back to the user's mobile device for display [51], [81]. The display of results and the overall solution can also take the form of a web-based application, which has an advantage in terms of use because no installation is required [43]. Luo et al. [88] proposed a collaborative edge-cloud architecture with optimized data management between the user's mobile device and the cloud server. The application developed by Li et al. [46] contains three main blocks: a mobile block for image capture, a cloud block on which the DL model runs, and a big data block for data collection.

3) OPERATING SYSTEM, HARDWARE AND HARDWARE PRICE

In the analyzed cases, solutions were primarily designed for the two most popular mobile operating systems: iOS and Android. Although most authors focused on deploying their solutions on a single OS, some authors (e.g., Wei et al. [71] and Majumder et al. [90]) developed cross-platform applications using the Keras deep learning framework [132], enabling deployment on both operating systems. There are also other deep learning frameworks that offer similar functionalities, but these are not the subject of this analysis. We also analyzed the hardware used with respect to the sensor intended to capture eye images. Due to significant differences between the mobile devices used by various authors, we did not pay special attention to specific models. The other monitored parameter was the estimated price of the designed hardware solution for scanning, excluding the price of a mobile device. We omitted this parameter due to price differences between individual models. However, it may not have any effect on the functionality of the proposed solution presented by the individual authors. The estimated price of the solution is only a rough estimate, as we obtained the prices from the manufacturer's websites and publicly available offers from various sellers. This estimate is only indicative and may differ significantly between individual sellers. The monitored parameters have an impact on the reproducibility of the results by other authors from the point of view of the continuation of the research, while the price and availability of the hardware solution used can be a limiting factor. The results of our analysis are shown in Appendix Tables 12-15. From the perspective of hardware procurement and related costs, the proposed solutions vary significantly. A review of 74 articles revealed that only four authors (approximately 5%) used a custom fundus attachment compatible with a smartphone camera for eye screening, which is a low-cost solution that typically costs less than $100. These attachments are often 3D printed or assembled from readily available components such as lenses and cameras. Such innovative and budget-friendly solutions do not pose barriers to immediate

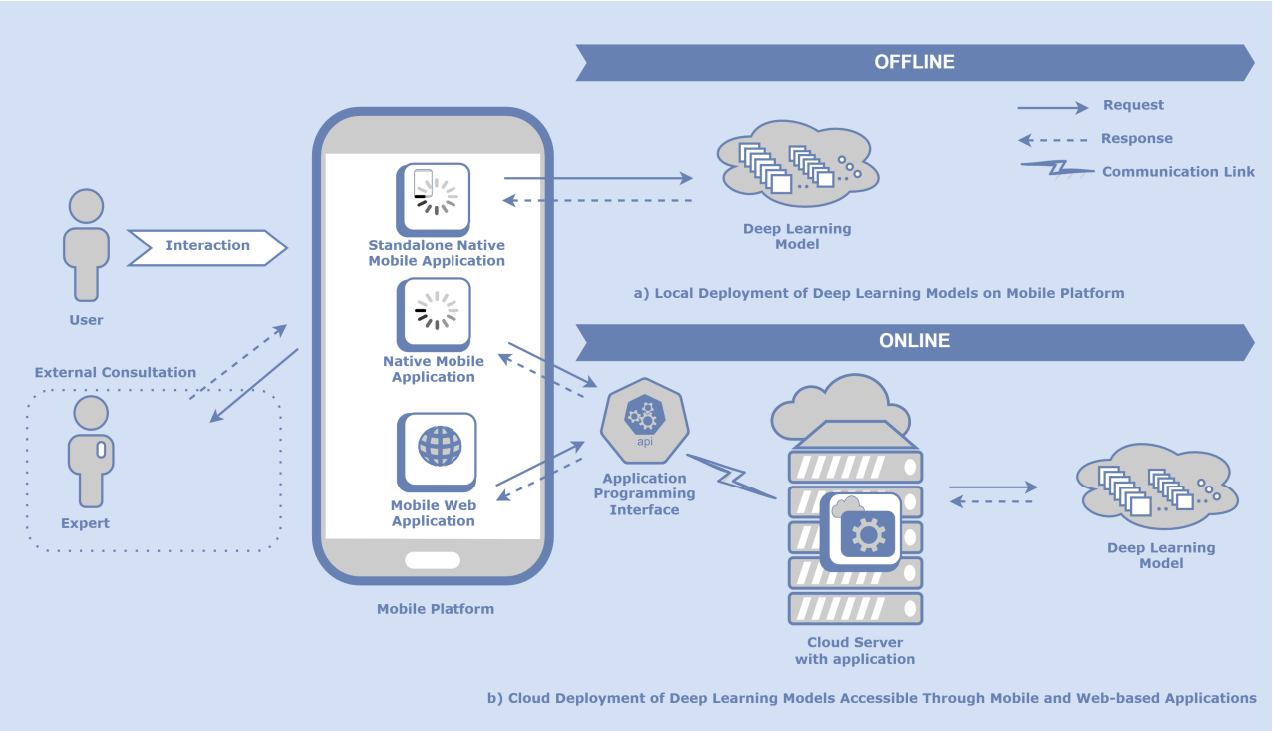

FIGURE 6. Local and cloud deployment of deep learning models accessible through mobile and web-based applications.

implementation, even in resource-limited conditions. The second most cost-effective approach employed by the four research teams (about 5%) involved using a standard digital camera priced between several hundred and a few thousand dollars to capture images to train deep learning models. Furthermore, thirteen authors (approximately 18%) used smartphone cameras directly without any special attachments. In terms of higher price, 22 authors (30%) adopted commercial professional solutions with costs estimated at thousands of dollars, which can act as a significant barrier to broader adoption by other research or medical teams. The hybrid approach, which combines the use of mobile devices with a mid-range attachment (costing hundreds to thousands of dollars), was chosen by the 13 authors (18%). This compromise balances cost and functionality, making it more accessible than commercial solutions while addressing some of the limitations posed by low-cost attachments. The remaining 18 authors (approximately 24%) did not use any hardware and relied on available data from public datasets.

4) SOLUTION AVAILABILITY AND REPRODUCIBILITY

The last monitored parameters in the analyzed articles were the availability of the solution in terms of the mobile application created, data, model, or source code. Reproducibility analysis (Tables 12-15 in the appendix) revealed that only four research teams (approximately 5%) of the 74 studied made their applications publicly available for download. One of them was the application only for data collection without interactive features. Furthermore, fourteen authors (19%) shared their training data, while seven authors (9%) provided access to trained models or complete source codes. Despite these efforts, significant challenges remain to ensure the reproducibility and accessibility of research outputs. The limited sharing of resources suggests that research can remain confined within individual labs or groups, making collaborative progress and innovation more difficult.

Examples of screenshot images of smartphone applications from reviewed articles are shown in Figure 7.

F. CLINICAL CONTRIBUTION OF SMARTPHONE IMAGING AND DEEP LEARNING DIAGNOSIS IN OPHTHALMOLOGY

Different ophthalmologic diagnoses are based on images of the anterior and posterior segments of the eye. Moreover, there are some specifics in the deep learning ophthalmologic image diagnosing compared to standard examination, e.g., the diagnosis of cataract, although anterior segment structure pathology could be made based on blurring of the captured fundus image [79], which is definitely not part of the standard examination process in the doctor's office. In addition, glaucoma diagnosis is always made based on the appearance of the optic nerve head on fundus photography when using a smartphone. However, the accuracy could be limited because of multimodal assessment requirements in glaucoma (intraocular pressure measurement, gonioscopy, visual field, optic nerve head, and retinal nerve fibre layer examination). On the other hand, the disease that can be found in the posterior segment could be screened using a smartphone

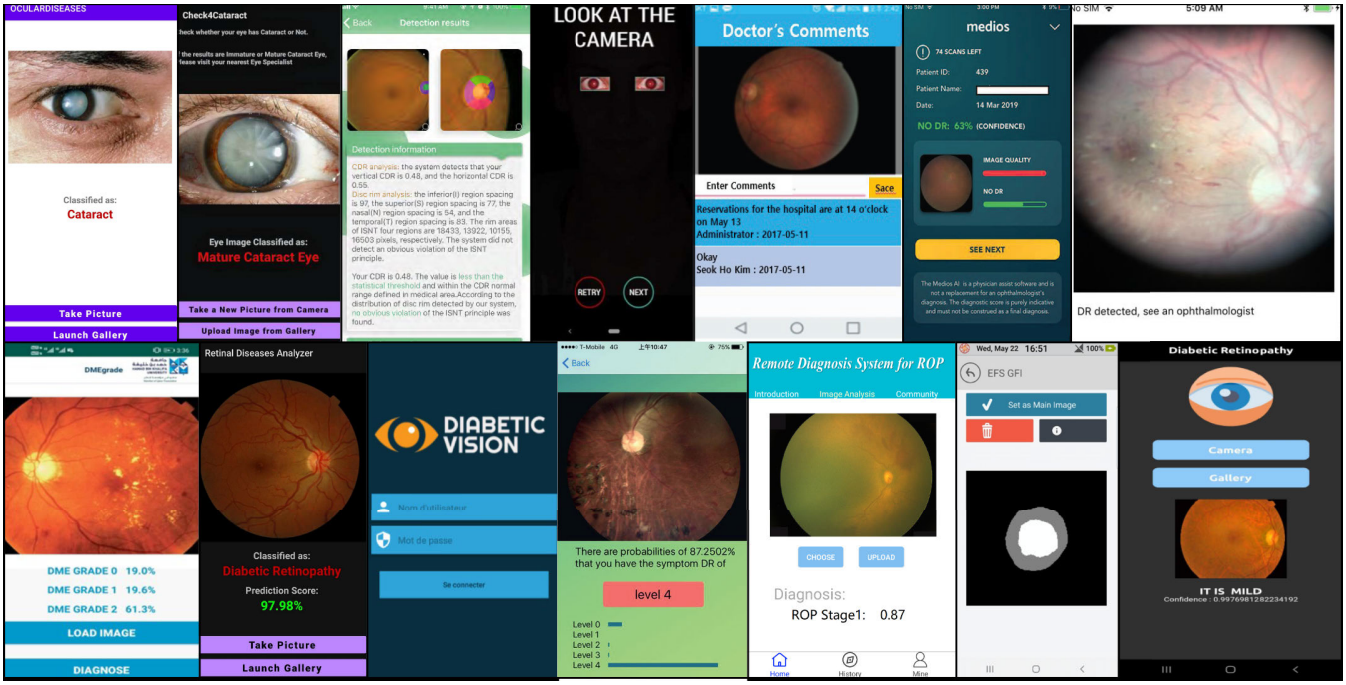

FIGURE 7. Examples of screenshot images of smartphone applications from reviewed articles.
First row (from left to right): [27], [28], [53], [61], [68], [71], [81], second row (from left to right): [75], [80], [85], [86], [88], [91], [94].

direct image, for example, to detect leucocoria [28]. The focused clinical entity also depends on the available capture technology and appropriate datasets. The graphical analysis of the focused clinical diagnoses in the anterior and posterior segment imaging is shown in Figure 8. Most of the articles are classifying cataract and diabetic retinopathy, in the imaging of the anterior and posterior segments, respectively. The following diagnoses are pterygium, ocular surface disease, conjunctivitis, keratitis in the anterior segment, and glaucoma in the posterior segment.

1) AI- ASSISTED SMARTPHONE DIAGNOSTICS USING ANTERIOR SEGMENT IMAGES OF THE EYE

Direct smartphone images are used mainly to detect anterior segment pathologies. The advantage is that there is no need for any smartphone attachment or device, and the image could be captured by the patient himself, sometimes with the assistance of another person. In addition, the resolution of actual smartphone photographs is high; therefore, small physiological or pathological details could also be noticed. If available, a smartphone-attached slit lamp can mimic standard anterior segment examination, providing some new perspective compared to standard two-dimensional direct photography of the eye.

Inflammations or other pathologies of the conjunctiva [27], [51] or cornea [35], [46], [58], including possible tumors [59] could be detected. From a clinical point of view, it is valuable to distinguish the etiology of keratitis – bacterial, fungal, or herpetic [58]. The ocular redness was detected by segmentation of the sclera (and also the conjunctiva) by [34] as part of the uveitis tracking system. Dry eye disease, which is a consequence of insufficient quantity or quality of patient tears, is a common cause of discomfort, sometimes also of loss of vision. The self-screening of ocular surface disease was proposed by [41]. Okazaki et al. [54] presented a non-conventional method using a grid-like cylinder containing a ring light that generates a concentric grid on the surface of the eye. The distortion of this grid is suspected to be due to contact lens-induced dry eye disease. Hong et al. [44] divided the dataset images into two classes based on the tear volume tests using a phenol red thread. An application that can distinguish between urgent and non-urgent anterior segment pathology could also be useful [29]. Although rare in developed countries, trachoma is one of the leading causes of irreversible blindness in developing countries. To classify trachoma, images of the tarsal conjunctiva were used in [50].

Zaki et al. [60] screened for keratoconus, the disease in which the cornea has a cone shape, from images captured from the side. Gairola et al. [31] used a smartphone-based corneal topographer that generated corneal heat maps.

The classification of the presence of pterygium was studied in 3 of the 74 articles [38], [39], [48].

In our reviewed articles, cataract was detected in two different sources of images. For cataract prediction, direct images were used mainly [33], [36], [37], [40], [53], [56]. Hu et al. [45] detected cataracts from slit lamp images connected to the smartphone.

In pediatric ophthalmology, it is important to detect visual impairment in children as soon as possible to prevent amblyopia. Smartphone applications could help parents screen their children for further examination when suspected. Murali et al.

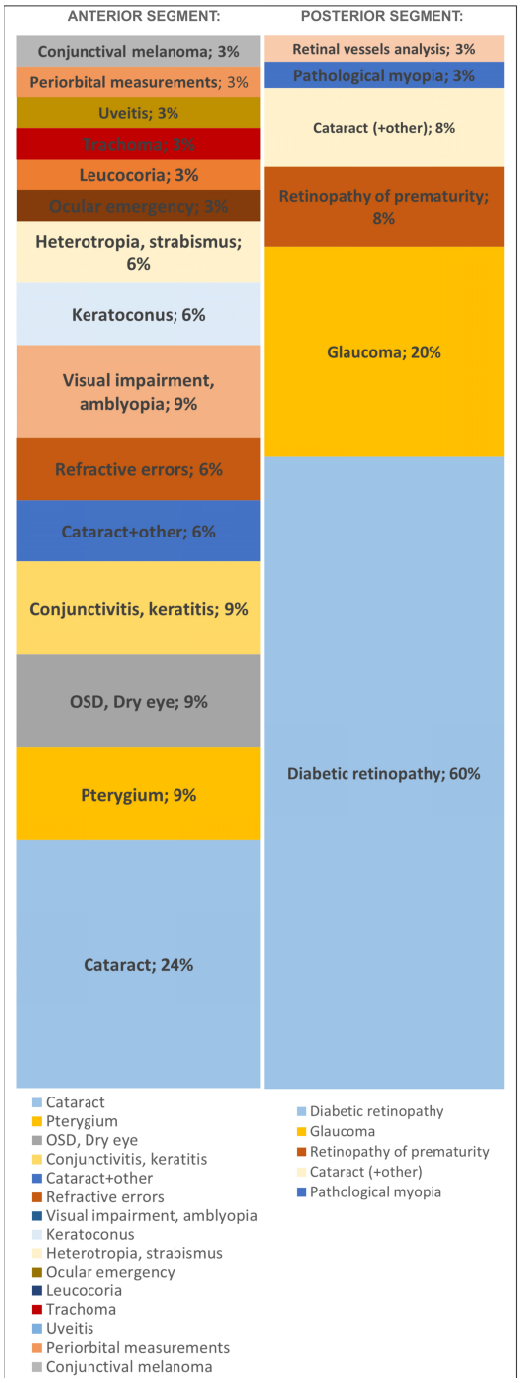

FIGURE 8. Ophthalmologic diseases diagnosed or screened in described complete and partial solutions.

[52] screened for amblyopia by observing refractive error and optical media opacities in the red reflex in the pupil. Chen et al. [29] detected visual impairment by various causes using a smartphone video of the child. Strabismus detection applications were proposed by de Figueiredo et al. [43] and Gupta et al. [32]. The appearance of the pupillary red reflex (pupillary crescents) could predict the spherical and cylindrical refractive power [47]. This observation is based on the red reflex test (Bruckner test).

Only 2 of 74 reviewed articles diagnosed tumors - Bernard et al. [28] classified direct smartphone images according to the presence of a red reflex to detect leukocoria and thus retinoblastoma. The second work by Yoo et al. [59] classified the presence of conjunctival melanoma on direct images. In rare diagnoses, such as retinoblastoma, false positives could exceed true positives, leading to the low sensitivity of such applications [28]. Smartphone diagnosis and screening for ophthalmologic tumors using deep learning, especially those in the anterior segment, is definitely an area of great uncovered potential, when there will be a larger smartphone-captured dataset available containing these pathological lesions [59].

Direct images of the eye focusing on the anterior segment could also be used for various measurements, in the periorbital region [57] and in the depth of the anterior chamber [55].

2) AI-ASSISTED SMARTPHONE DIAGNOSTICS USING POSTERIOR SEGMENT IMAGES OF THE EYE

Various retinal diseases could be screened by examining the posterior segment using smartphone deep learning methods. As we described earlier, due to the inability to capture the posterior segment of the eye directly using smartphones, many fundus attachments and devices are used. To detect retinopathy of prematurity (ROP) in remote and low-resource environments, smartphone solutions are favorable [88], [93], [98]. A comprehensive system to detect ROP and classify its severity into three classes was proposed by [88]. The classification into plus or non-plus disease was presented by [98].

One of the leading causes of blindness, diabetic retinopathy (DR), is also the leading disease in smartphone deep learning ophthalmologic applications. Twenty-four of the works focus on DR (12 in complete and 12 in partial posterior segment solutions). Binary classification (also suitable for screening) can divide images into healthy (without DR) and with DR, or alternatively, referable (healthy and mild non-proliferative DR) and unreferable (moderate and severe non-proliferative with proliferative DR and/or diabetic macular oedema (DME)). The classification into DR or non-DR or referable or non-referable DR was proposed by [67], [68], [69], [70], [71], [73], [80], [86], [87], [90], and [99]. The three-class classification into normal, non-proliferative, and proliferative was described by [92]. The classification into more stages was proposed by [10], [61], [73], [77], [82], [83], [86], [90], and [97], mainly into five stages: mild, moderate, and severe non-proliferative DR, and proliferative DR. The prediction of the grade of diabetic macular oedema was proposed by [75]. Some solutions use commercially available Remidio MEDIOS AI with EyeArt software, automated offline analysis of retinal images captured using the Fundus on Phone handheld retinal camera [62], [63], [66]. This solution identifies DR, referable DR or worse, and/or DME.

The other commercially available smartphone system used was EyerCloud by Phelcom Technologies LLC [69], [70].

Another leading cause of blindness, AMD, was not analyzed in any reviewed article, which was really unexpected, because many patients suffer from this diagnosis, and such a smartphone application could be demanding.

Although it is not a retinal disease, glaucoma is often diagnosed using a photograph of the fundus captured with a smartphone [81], [89], [95]. Optic disc-centered fundus images are captured in [64], [65], [78], and [96]. The segmentation of the optic disc and the cup was proposed by [81], [91], [96] to visually represent the cup-to-disc ratio of the optic nerve head. The commercially available solution from the same company as in DR detection, Remidio MEDIOS, Fundus on phone handheld retinal camera, together with AI Glaucoma software, was presented by [64], and [65].

As mentioned above, cataract can also be diagnosed by detecting blurring of the fundus image [79]. As the lens becomes less transparent, we could expect a lower quality of fundus imaging.

As part of the diagnostics from fundus images, other pathological entities were also screened, ie, pathological myopia [76].

IV. DISCUSSION

Smartphone-based deep learning imaging diagnostics have significant potential to revolutionize screening for sight-threatening eye diseases. Analyzed solutions offer several advantages: they are relatively inexpensive, accessible, portable, and require minimal computing resources. In addition, they improve diagnostic availability and reduce the need for specialized personnel.

Deep learning technology enables efficient mass screening and accelerated decision-making in ophthalmology. Smartphone applications leverage these advances, enabling earlier diagnosis and thus improving treatment outcomes, depending on the integration of current medical knowledge with the technological capabilities of smartphones. Technological innovations such as specialized chips (e.g., GPU, NPU) increase device performance and enable the deployment of complex models. However, limitations arise from constraints on mobile computing that require the use of simplified deep neural network architectures. Smartphone-based deep learning applications are ideal for implementation in resource-constrained settings. The ethical and regulatory challenges surrounding the deployment of AI-based tools on smartphones in developing regions cover several areas. Health and biometric data must be collected and stored, but many regions lack adequate data protection laws. Poor internet connectivity, limited access to updates, and the absence of local technical expertise can limit available solutions and increase the risk of misdiagnosis due to outdated algorithms. Additionally, local populations may differ ethnically and demographically from those represented in training datasets, making local validation essential. Furthermore, even in developed countries, deep learning tools for smartphones can enhance rapid clinical decision-making, potentially leading to earlier treatment initiation.

The process of capturing images of the eye using a smartphone is highly dependent on the specific ocular structures that are being examined. Capturing the anterior segment images typically does not require any additional hardware beyond the built-in camera of the smartphone, and it is accessible to every smartphone user, even as a selfie. However, it is very important that the image is of sufficient quality, does not contain motion blur, is sharp, the eye is not covered, and is captured in the desired resolution, and any other specific imaging criteria are met. These can be incorporated into the smartphone application in the form of image quality tests immediately after the image is captured, resulting in increased reliability [30]. In general, images of the anterior segment captured by a smartphone often match the quality of standard cameras, offering significant diagnostic potential. Although current reviewed applications have not fully embraced this capability, there is great promise in the future for creating high-quality public datasets of anterior segment pathologies. However, the built-in camera is not the only integrated component that could be useful for anterior segment analysis. The built-in Light Detection and Ranging (LiDAR) sensor, available in some smartphones, shows promise for mapping the ocular surface, including detecting corneal abnormalities in the future. On the other hand, the safety of directing LiDAR light toward the eye raises potential concerns; however, ocular damage is unlikely in actual settings, as the emitted light is dispersed over a broad area and is not intended for direct ocular exposure.

Posterior segment imaging with smartphones requires special attachments or devices, including a magnifying lens, and also the second person's assistance with some training or experience with such solutions. The quality of captured images varies widely depending on the add-on used, ranging from low-cost 3D printed attachments to expensive, complex commercial devices with AI capabilities. Despite these drawbacks, these solutions are compact, accessible, and affordable compared to standard fundus cameras, making them suitable for mobile or on-the-go screenings.

Different light conditions, various distances, and the addition of more gazes can be valuable when capturing the images of the anterior segment directly. In addition, to capture fundus or red reflex photography, some built-in camera settings in smartphones could make it challenging. Most devices use a pre-flashlight directly into the eye or post-processing algorithms to remove the red reflex. These prefabricated settings are not easy to change, although some studies have reported that they successfully did [28], [52]. However, these methods are not well documented or standardized, making these solutions unreproducible. Although fundus or red reflex photography requires a dilated pupil, some smartphone models allow image capture in non-mydriatic mode without significantly compromising the captured field of view [10], [61], [62], [63]. The need for

medicamentous pupil dilation could then be bypassed by using near-infrared light (NIR) or by specific changes in capturing light and distance. NIR illumination modules are already integrated into iPhone and Android smartphones to unlock the phone using facial recognition.

When we analyzed deep learning models, we found the dominance of ResNet and Inception architectures, in addition to MobileNet in posterior segment solutions, probably because of the more frequent presence of applications with inference requiring model deployment into smartphones, suggesting that smartphone deployment requirements heavily influence model selection across analyzed solutions.

Training deep learning models typically requires large datasets. Currently, in the solutions analyzed, there are only two publicly available datasets for smartphone-based ophthalmic imaging: the Brazil glaucoma dataset captured using Welch Allyn handheld ophthalmoscope [78] and the Cataract Mobile Periocular Database [105]. In addition, some datasets contain both standard fundus camera images and smartphone-captured images. It is important to note that images from standard fundus cameras generally have a higher resolution and a wider field of view compared to those captured by smartphones. Training of models using publicly available non-smartphone data for testing on smartphone images is not uncommon, but might not be sufficient in the case of testing images captured by smartphones. There is a critical gap in publicly available high-quality smartphone datasets, even in anterior segment datasets, which could be captured directly without the need for any attachment. This impedes the reproducibility and standardization of such applications and slows their further development and availability. The disparity in image quality between smartphones and standard fundus cameras can be addressed through image enhancement techniques and data augmentation. In addition, collecting more data from video sequences recorded by smartphones [60], [87] can help expand the dataset. The lack of public datasets tailored for smartphone-based ophthalmic imaging and their differences from those captured by standard fundus cameras may significantly hinder the development and practical applications of deep learning models in this field.

From a technical perspective, mobile applications can be divided into two groups: offline applications that allow the deployment of pre-trained deep learning models directly on smartphones without internet access, and online applications that rely on cloud servers for the computational offloading, usually in the form of a native mobile or web application. Of the total number of 74 analyzed solutions, only 19 were online applications, which represents approximately 26 percent. One of the reasons is certainly the added complexity in creating online applications, as well as the increased security demands due to privacy concerns [27]. For offline solutions, authors generally avoid this topic and focus more on the implementation description and technical parameters such as the inference time or latency for a given neural network. Although these are important technical parameters and there is some trade-off between offline evaluation, which typically takes less than 1 second, and cloud-based online solutions, where evaluation typically takes less than 1 minute, they are not critically important. However, the authors very rarely address the topics of portability of the solution to other devices, energy efficiency, thermal constraints, or regulatory considerations. In this area, commercial solutions are much more advanced and ready for clinical adoption, as they usually have the necessary certifications and meet regulatory requirements. Therefore, it is not surprising that some of them have been used by authors in both offline (e.g., Medios AI) [64], [65] and online analyzed solutions (e.g., EyeArt) [66], [67]. However, expensive commercial devices designed for the capture of fundus images can be a barrier because of their high cost. In addition to our specific findings, the broader trend we identified is that authors are focusing on affordable fundus imaging setups. This includes systems combining mobile phones with commercial mid-price eye scanning attachments and parallel developments of low-cost hardware using 3D printing.

From a clinical perspective, deep learning smartphone diagnostics have specific nuances that differ from traditional examination methods. The focus lies on two main factors: the technology used for image capture and the availability of suitable datasets. For example, cataract diagnosis can be performed by analyzing direct images of the pupil to identify mature cataracts or by assessing the quality of fundus images, which may be worsened by lens opacity. In addition, certain pathologies of the posterior segment can be identified if the red reflex is not present (ie, mature cataract or leukocoria in retinoblastoma). Intraocular pressure (IOP) cannot currently be measured using a smartphone, but glaucoma can be diagnosed by evaluating changes of the optic nerve head visible in fundus images; however, we cannot expect high precision, because the diagnosis of glaucoma traditionally requires a multimodal assessment. On the other hand, diabetic retinopathy appears to be more suitable for smartphone screening: the diagnosis is based primarily on fundus findings. That explains the primary focus on DR in posterior segment solutions, which also contains articles classifying the severity of the disease and available commercial solutions (e.g., Medios, EyeArt).

In our analysis of anterior segment disease applications, we observed a focus on conditions such as pterygium, conjunctivitis, keratitis, eyelid tumors, and keratoconus. However, there are numerous other diagnoses that could be effectively screened using smartphones, yet they remain underrepresented in the reviewed literature. Conditions such as eyelid inflammations and pathologies, corneal dystrophies, endocrine orbitopathy, and iris tumors are examples of these areas not covered. In particular, pterygium, which is not a sight-threatening condition, is addressed in three of the reviewed articles ([38], [39], [48]), contrasting with ocular tumors, which are rarely diagnosed using deep learning on smartphones ([28], [59]), despite their life-threatening nature. In remote and low-resource environments, the detection

of retinopathy of prematurity using smartphones could be advantageous ([88], [93], [98]). In developed countries, screening for conditions such as the epiretinal membrane or macular hole may be beneficial; however, screening for retinal detachment may present a particular challenge due to its often peripheral onset, making early diagnosis using smartphones nearly impossible due to the limited field of view.

Screening of rare diseases may remain a challenge: there is usually a lack of datasets with labeled data, classes could be imbalanced if present in datasets with multiple diseases, or too heterogeneous if combined from multiple datasets. Insufficient data may then lead to a high rate of false positives, because models tend to overfit or fail to recognize subtle patterns. There are several strategies to bypass these potential problems, such as various data augmentation techniques, including synthetic data generation, weighted loss function training, or federative learning allowing collaborative model training across more institutions.

Interestingly, age-related macular degeneration (AMD), another leading cause of blindness, was not analyzed in any of the reviewed articles. This could be caused by the lower accessibility of public datasets with AMD, compared to DR. Some datasets are available on academic request (i.e. AREDS [133]), some like ODIR [134] contain AMD together with other diseases, and the number of images is small, so they need to be concatenated, and finally there were not as many active AMD challenges, as we observed with DR. It is also difficult to find any AMD fundus datasets review article.

In standard clinical practice, diagnostic conclusions usually integrate the findings of multiple examinations. In contrast, smartphone-based screening solutions often rely on a single modality, such as one image or one measured parameter. Consequently, the sensitivity and specificity achievable from a single input are inherently limited and must be validated under real-world clinical conditions against reference diagnoses; confirmatory testing using clinical gold standards remains essential. For diseases such as diabetic retinopathy, in which the diagnosis is based primarily on fundus findings, higher diagnostic accuracy can be anticipated. However, in conditions such as glaucoma, where the evaluation of the optic nerve head constitutes only one component of the evaluation, a multimodal approach incorporating additional tests (e.g., perimetry, OCT) is essential. In such cases, results equivalent to comprehensive clinical examinations should not be expected, and future approaches should integrate multiple data sources as input. New hardware innovations, such as portable augmented and virtual reality (AR and VR) perimetry devices, could potentially serve as another convenient glaucoma screening input—either for use on the go or for home-based screening.

Although we did not perform a direct head-to-head comparison in this study, cost analyses from similar implementations indicate substantially reduced per-patient screening costs. Telemedicine-based screening for diabetic retinopathy has been shown to significantly reduce costs, particularly in low-income and rural populations with high transportation expenses [135], and to lower costs even in developed countries, supporting the expansion of tele-ophthalmology programs, including for follow-up examinations [136]. Evidence from other studies further suggests that incorporating artificial intelligence into screening workflows can improve cost-effectiveness compared to conventional ophthalmologist-based screening [137]. Moreover, screening without direct specialist involvement has demonstrated both reduced costs and promising accuracy in diabetic retinopathy detection [138]. Therefore, the current literature supports the use of smartphone-based deep learning solutions in ophthalmology, not as a replacement for comprehensive clinical evaluation, but as a complementary first-line screening tool.

A key element of these solutions is the incorporation of explainable artificial intelligence (XAI), which refers to methods and techniques that make the internal workings and decisions of deep learning models understandable and interpretable by humans. The explanation mechanism translates complex model reasoning into a digestible format suitable for typical clinical workflows, which most often involve various forms of visualization, such as class activation mapping (CAM), saliency maps depicting relevant image regions, or even text summaries. XAI integration is inherently linked to model accountability, ensuring that creators and developers of an AI system can be held accountable for its performance and potential harm. Therefore, careful adoption is needed, and common practice is to deploy such systems in the form of decision support systems that require the verification of results by a physician.

Besides the emerging need for new public smartphone datasets creation and integration of XAI, a roadmap for future solutions development in this area could be inspired by our TRIPOD-AI-based evaluation score, to fulfill our proposed criteria (Table 1). Determining the standard capturing methodology for each solution could help reproducibility, but it could be complicated to create general standards for eye smartphone imaging due to the diversity between devices. Another drawback of reviewed smartphone applications is the focus on one specific ophthalmologic condition. These solutions usually handle a single eye pathology, which means that multiple of them would be needed to cover the full ophthalmologic disease spectrum, leading to limited clinical complexity. Therefore, developers of future applications should focus on more complex deep learning smartphone applications that diagnose multiple pathologies. In addition, many of these reviewed applications are experimental and are not available to the public for use or testing in real-world settings. This makes current evaluations of their clinical implementation insufficient.

V. CONCLUSION

Smartphone applications that can be used to improve the diagnostic process and management of various sight-threatening conditions are in high demand. We reviewed the use

of deep learning ophthalmologic smartphone applications, focusing on the imaging techniques, used hardware, and datasets, deep learning network architectures, and their implementation. The described applications were analyzed to provide guidance to ophthalmologists and technicians in this new interdisciplinary research field. We described various methods and approaches for smartphone ophthalmologic image capture and hardware and software solutions, highlighting the advantages and disadvantages that occur in practice.

A limitation of the presented review is the restricted scope of the reviewed applications and issues with their availability, as most of them are experimental. Current smartphone applications often focus on specific ophthalmological pathologies, such as diabetic retinopathy. The handling of multiple conditions requires separate applications for different diseases, which is impractical for comprehensive clinical use.

While analyzed mobile applications may offer decent performance suitable for triage or initial assessment, especially when designed to meet certain accuracy benchmarks, they may lag behind established gold standard tools in terms of peak sensitivity and specificity reported across studies simulating clinical practice. Mobile applications excel in accessibility and integration potential into existing healthcare structures for primary care or community screening programs, where immediate high-accuracy AI assistance is not the only consideration; ease of deployment on widely available smartphones makes them highly flexible and cost-effective outside traditional ophthalmology settings. Although smartphones have great potential to advance ophthalmic imaging, significant challenges remain in terms of clinical validity, practicality, and implementation. Addressing these challenges through collaboration will be key to maximizing the impact on global eye health care.

APPENDIX

See Tables 8 to 15.

TABLE 8. Summary of anterior segment COMPLETE SOLUTIONS, used datasets, best performed deep neural networks, solved tasks with best results.

Used datasets	Baseline deep NN	Task (Disease)	Best results	First author [reference]
own-SP	CNN	classification cataract/conjunctivitis/ healthy (CATARACT+ OTHER)	98.58% (Acc.) 99% (Sens.) 94% (Spec.)	Baig [27]
own-SP	ResNet	classification of leucocoria/ normal (LEUCOCORIA)	87% (Sens.) 73% (Spec.) 0.93 (AUC-ROC)	Bernard [28]
own- SP own-slit-lamp	DenseNet201	classification urgent/semiurgent/ nonurgent (OCULAR EMERGENCY)	80.8% (Acc.) 0.982 (AUC)	Chen J [29]
own- SP	EfficientNet- B2	facial landmark localization with quality control detection (VISUAL IMPAIRMENT, AMBLYOPIA)	0.843 (AUC) 82.6% (Acc.) 80.9%(Sens.) 83.5% (Spec.)	Chen W [30]
own-standard corneal topograph own- SP corneal topograph	dual-head CNN (ResNet34 backbone)	classification of keratoconus/ non- keratoconus (KERATOCONUS)	93.1% (Acc.) 91.3% (Sens.) 94.2% (Spec.)	Gairola [31]
own- SP	ConvNet	4-class classification of heterotropia types (HETEROTROPIA, STRABISMUS)	85.72% (Acc.) 86.67% (Sens.) 83.55% (Spec.)	Gupta H [32]
Kaggle own- SP	SDLM	classification of healthy/ cataract (CATARACT)	93.44% (Acc.)	Neogi [33]
Sclera Blood Vessels, Periocular and Iris (SBVPI) [120] own-SP	U-net	sclera segmentation (UVEITIS)	N/A	Perera [34]
own-slit lamp own- SP	YOLO V.5	9-class classification of corneal diseases and cataract triage classification urgent/ semi-urgent/ routine (CATARACT+ OTHER)	0.931-0.998 (AUC) 62.8-95.8% (Sens.) 96.9-99.8% (Spec.)	Ueno [35]
own-SP	CNN	classification normal/ cataract cataract grading (CATARACT)	96% (Sens.) 25% (Spec.) 88% (Acc.)	Vasan [36]
Cataract Mobile Periocular Database (CMPD) [105] own- SP	MobileNetV3Small	classification normal/ cataract (CATARACT)	98,67% (Acc.) 100% (Sens.) 98,18% (Spec.)	Verma [37]

- "SP"- smartphone,"NN"- neural network, "CNN"- Convolutional Neural Network, "Acc."- Accuracy, "Sens."- Sensitivity, "Spec."- Specificity, "AUC"- Area Under the Curve, "N/A"- Not available

TABLE 9. Summary of anterior segment PARTIAL SOLUTIONS, used datasets, best performed deep neural networks, solved tasks with best results.

Used datasets	Baseline deep NN	Task (Disease)	Best results	First author [reference]
own, based on Pterygium-Net [139]	Densely connected DeepLab	pterygium segmentation (PTERYGIUM)	92.02% (Acc.) 83.81% (IOU)	Abdani 2020 [38]
own, based on Pterygium-Net [139]	Group-PPM-Net (inspired by FC-Dense-Net)	pterygium segmentation (PTERYGIUM)	91.17% (Acc.) 86.69% (IOU)	Abdani 2021 [39]
public dataset	NasNetMobile	classification cataract/ non-cataract (CATARACT)	99,47% (Acc.)	Charan [40]
own- SP	DenseNet	classification ocular surface disease/ normal (OSD,DRY EYE)	90.56% (Acc.)	Chen R [41]
own- SP	ResNet 18	refraction probabilities prediction (VISUAL IMPAIRMENT, AMBLYOPIA)	81,6% (Acc.)	Chun [42]
own- DC	ResNet-50	9-class classification of eye versions to gazes (HETEROTROPIA, STRABISMUS)	42-92% (Acc.)	de Figueiredo [43]
own- SP	ResNet50	classification of normal/ dry eye (OSD,DRY EYE)	75% (Acc.)	Hong [44]
own- SP+ slit-lamp	ShuffleNet+SVM	classification of pronounced cataract/ early cataract/ non- cataract (CATARACT)	93.48% (Acc.) 89.2% (Sens.) 97.37% (Spec.)	Hu [45]
own- slit lamp own- SP	DenseNet121	classification of normal/ keratitis/ other (CONJUNCTIVITIS, KERATITIS)	99.8% (AUC) 97.7% (Sens.) 98.2% (Spec.)	Li Z [46]
own-SP	AI platform MedicMind: Inception V3	multi-class classification of spherical power (REFRACTIVE ERRORS (MYOPIA))	75% (Acc.)	Linde [47]
own-slit-lamp own-SP	Faster RCNN (based on ResNet 101)	pterygium detection and grading (PTERYGIUM)	93.6% (Sens.) 96.13% (Spec.) 92.38% (Acc.) 0.9426 (AUC)	Liu [48]
own- slit-lamp	ResNet 101	classification congenital cataract intervention/ nonintervention (CATARACT)	99.1% (Sens.) 99.4% (Spec.) 0.996 (AUC)	Long [49]
dataset from clinical trial in Niger and Ethiopia [140]	Google Cloud AutoML Vision	classification of normal/ intense trachomatous inflammation (TRACHOMA)	95% (Sens.) 92% (Spec.) 93% (Acc.)	Milad [50]
own- from internet	EfficientNet	classification of normal/ conjunctivitis (CONJUNCTIVITIS, KERATITIS)	84%(Acc.)	Mukherjee [51]
own- SP	CNN	detection iris ladmarks (VISUAL IMPAIRMENT, AMBLYOPIA)	N/A	Murali [52]
public dataset, own ground truth	MobileNetV2	classification of cataract mature/ immature/ healthy (CATARACT)	94.8% (Acc.)	Nair [53]
own- SP with grid-like cylinder and ring light	ResNet50	classification dry eye/ healthy (OSD, DRY EYE)	95% (Acc.)	Okazaki [54]
own- SP+ slit-lamp	ResNet34	anterior chamber depth prediction (REFRACTIVE ERRORS (MYOPIA-ACD)	N/A	Qian [55]
own- SP	ResNet50	classification cataract/ normal (CATARACT)	98% (Acc.) 97.8% (Sens.) 98.1% (Spec.) 0.999 (AUC-ROC)	Ramlan [56]
own- SP	ResNet50, U-net style upscaling	iris, eye aperture, eyebrow segmentation (PERIORBITAL MEASUREMENTS)	0.96 (Dice koef.), 0.9 (Dice koef., 0.82 (Dice koef.)	Van Brummen [57]
own- slit lamp own- SP	InceptionV3	classification of normal/ bacterial keratitis/ fungal keratitis/ herpes simplex virus stromal keratitis (CONJUNCTIVITIS, KERATITIS)	0.9588 (AUC)	Wang [58]
own- from internet	MobileNetV2	classification of melanoma/ other (CONJUNCTIVAL MELANOMA)	97.2% (Acc.) 0.983% (AUC)	Yoo [59]
own- SP	VGG16	classification normal/ keratokonus (KERATOCONUS)	95.75% (Acc.) 92.25% (Sens.) 99.25% (Spec.)	Zaki [60]

- "SP"- smartphone, "NN"- neural network, "CNN"- Convolutional Neural Network, "DC"- Digital camera, "Acc."- Accuracy, "Sens."- Sensitivity, "Spec."- Specificity, "AUC"- Area Under the Curve, "N/A"- Not available,"IOU"- Intersection Over Union, "OSD"- Ocular Surface Disease

TABLE 10. Summary of posterior segment COMPLETE SOLUTIONS, used datasets, best performed deep neural networks, solved tasks with best results.

Used datasets	Baseline deep NN	Task (Disease)	Best results	First author [reference]
own- SP Remidio fundus camera Diabetic retinopathy detection (EyePACS) [107]	InceptionV3	classification of DR refferable/nonrefferable (DIABETIC RETINOPATHY)	100% (Sens.) 89.55% (Spec.) 81.4% (Sens.) 91.5% (Spec.) 0.9648 (AUC) 100% (Sens.) 88.4% (Spec.) 98.84% (Sens.) 86.73% (Spec.)	Jain [62] Kemp [63] Natarajan [61] Sosale [10]
own- SP Remidio fundus camera	Feature Pyramid Network (ResNet50 backbone)	disc and cup segmentation classification no-referable/ referable glaucoma (GLAUCOMA)	93.7% (Sens.) 85.6% (Spec.) 89.3% (Acc.) 95% (LoA)	Rao [64] Shroff [65]
own- SP Remidio fundus camera	EyeArt® AI Framework	classification of DR sight-threatening/not-sight threatening (DIABETIC RETINOPATHY)	99.1% (Sens.) 80.4% (Spec.)	Rajalakshmi [66]
own- SP+ RetinaScope	EyeArt® AI Framework	classification of DR referrable/nonreferrable (DIABETIC RETINOPATHY)	77,8%(Sens.) 71,5% (Spec.)	Kim T [67]
Diabetic retinopathy detection (EyePACS) [107]	Exception-V3	classification of DR/ normal (DIABETIC RETINOPATHY)	N/A	Kim W [68]
own- SP+ Eyer	EyerCloud (Xception)	classification of DR less than mild NPDR/ more than mild NPDR (DIABETIC RETINOPATHY)	97.8% (Sens.) 61.4% (Spec.) 0.89 (AUC)	Malerbi [69]
Diabetic retinopathy detection (EyePACS) [107] own- SP	Xception	classification of DR less than mild NPDR/ more than mild NPDR (DIABETIC RETINOPATHY)	93.6% (Sens.) 71.7% (Spec.) 86.4% (AUC)	Penha [70]
Diabetic retinopathy detection (EyePACS) [107] STARE [121] own- SP+ D-Eye	Xception	classification of DR / not DR (DIABETIC RETINOPATHY)	94.6% (Acc.)	Wei [71]
own- SP+Volk-inView	NasNet Mobile	feature extraction in DR stages classification (DIABETIC RETINOPATHY)	95.91% (Acc.) 94.44% (Sens.) 96.92% (Spec.)	Elloumi 2022 [72]
Diavision, Diavision portable Messidor [113]	VGG16	classification of DR/ normal (DIABETIC RETINOPATHY)	100%	Alves [73]
DIARETDB0 STARE [121] own- SP+microscopic lens	Multi Layer Perceptron	classification of normal/ abnormal (CATARACT+ OTHER)	>87,5% (Acc.)	Bourouis [74]

- "SP"- smartphone, "NN"- neural network, "CNN"- Convolutional Neural Network, "Acc."- Accuracy, "Sens."- Sensitivity, "Spec."- Specificity, "AUC"- Area Under the Curve, "N/A"- Not available

TABLE 11. Summary of posterior segment PARTIAL SOLUTIONS, used datasets, best performed deep neural networks, solved tasks with best results.

Used datasets	Baseline deep NN	Task (Disease)	Best results	First author [reference]
IDRiD [111]	DenseNet-121	classification- DME grade 0/ grade 1/ grade 2 (DIABETIC RETINOPATHY (DME))	N/A	Al-Absi [75]
PALM challenge [116]	MobileNetV3 small	classification pathological myopia/ normal (PATHOLOGICAL MYOPIA)	0.9927 (AUC)	Ali [76]
Diabetic retinopathy detection (EyePACS) [107]	MobileNet ResNet 50	5-class classification of DR stages (DIABETIC RETINOPATHY)	76% (Acc.) 89% (Acc.)	Bidari [77]
own- SP- Brazil Glaucoma dataset	Ensemble	classification of glaucoma/ normal (GLAUCOMA)	90.0% (Acc.) 85% (Sens.) 96% (Spec.)	Braganca [78]
Kaggle "cataract dataset" ODiR [114]	MobileNet-V2	features extraction in cataract stages classification (CATARACT+ OTHER)	90.68% (Acc.) 91.43% (Sens.) 89.58% (Spec.)	Elloumi 2021 [79]
Diabetic retinopathy detection (EyePACS) [107]	Inception-V3	classification of DR/ no DR (DIABETIC RETINOPATHY)	92.51% (Sens.) 91,35% (Spec.)	Ghouali [80]
own- FC ORIGA [115]	U-Net	segmentation of optic disc and cup (GLAUCOMA)	76.42% (Acc.) 76.25% (Sens.) 76.51% (Spec.)	Guo [81]
Diabetic retinopathy detection (EyePACS) [107] APTOS 2019 Blindness Detection [106]	DCNN	5-class classification of DR stages (DIABETIC RETINOPATHY)	99% (Acc.) 97.5% (Sens.) 99.3% (Spec.)	Gupta S [82]
Diabetic Retinopathy Detection (EyePACS) [107]	Inception	5-class classification of DR stages (DIABETIC RETINOPATHY)	99.86% (Acc.) 99.25% (Sens.) 99.6% (Spec.)	Hagos [83]
own- SP+ Welch Allyn panoptic ophthalmoscope	U-net	retinal vessels segmentation (RETINAL VESSELS ANALYSIS)	N/A	Hu [84]
HRF [110] IDRiD [111] ODiR [114]	MobileNetV2	classification cataract/ glaucoma/ DR/ normal (CATARACT+ OTHER)	100% (Acc.)	Intaraprasit [85]
Diabetic retinopathy detection (EyePACS) [107]	Deep CNN	5-class classification of DR stages (DIABETIC RETINOPATHY)	86.17% (Acc.)	Li YH [86]
Diabetic retinopathy detection (EyePACS) [107] APTOS 2019 Blindness Detection [106] own- SP+EyeGo	DenseNet 201	classification of DR referrable/nonreferrable (DIABETIC RETINOPATHY)	89% (Sens.) 83% (Spec.)	Ludwig [87]
own- FC	ResNet101	classificaton of ROP normal/Stage 1/ 2/ 3 and above (ROP)	75%(Acc.) 60% (AUC)	Luo [88]
own-SP	CNN	classification glaucoma/nonglaucoma (GLAUCOMA)	85.9% (Acc.) 88% (Sens.)	Maddala [89]
Diabetic retinopathy detection (EyePACS) [107] APTOS 2019 Blindness Detection [106]	Inception-V3	5-class classification of DR stages (DIABETIC RETINOPATHY)	88.5% (Acc.)	Majumder [90]
ORIGA [115] Drishti-GS [109] REFUGE [117] RIM-ONE r3 [119] RIGA [118]	GFI-C-InceptionV3	classification of glaucoma/ no- glaucoma (GLAUCOMA)	90% (Acc.) 80% (Sens.) 94% (Spec.) 0.93 (AUC)	Martins [91]
APTOS 2019 Blindness Detection [106]	EfficientNet-B0	classification of DR no DR/ NPDR/ PDR (DIABETIC RETINOPATHY)	91.85% (Acc.)	Matthew [92]
own- SP Kaggle(not spec.)	U-net	Classification ROP/ normal (ROP)	98.07% (Acc.) 85.5% (Sens.) 83.4% (Spec.) 0,9807 (AUC)	Mutua [93]
Kaggle APTOS 2019 Blindness Detection [106]	MobileNet	5-class classification of DR stages (DIABETIC RETINOPATHY)	90% (Acc.) 91% (Sens.)	Nage [94]
own- FC own- SP+D-Eye	ResNet34	classification normal/ glaucoma (GLAUCOMA)	64.4% (Sens.) 85% (Spec.) 0.842 (AUC)	Nakahara [95]
RIM-ONE r3 [?] DRISHTI-GS [109] REFUGE [117] own- SP+ D-Eye	Inception ResNet V2	classification normal/ glaucoma (GLAUCOMA)	87% (Acc.) 47% (Sens.) 94% (Spec.)	Neto [96]
APTOS 2019 Blindness Detection [106]	EfficientNetB7 + VGG-16	5-class classification of DR (DIABETIC RETINOPATHY)	91.8% (Acc.)	Shrimali [97]
own- SP+ Volk 28D lens	GoogLeNet	classification of ROP „plus“/“non-plus“ (ROP)	96% (Acc.) 71.43% (Sens.) 100% (Spec.) 0.9834 (AUC)	Subrammaniam [98]
Diabetic retinopathy detection (EyePACS) [107]	MobileNets	classification of DR/ normal (DIABETIC RETINOPATHY)	73.3% (Acc.) 74,5% (Sens.) 63% (Spec.)	Suriyal [99]

- "SP"- smartphone, "NN"- neural network, "CNN"- Convolutional Neural Network, "DR"- Diabetic retinopathy, "ROP"- Retinopathy of prematurity, "Acc."- Accuracy, "Sens."- Sensitivity, "Spec."- Specificity, "AUC"- Area Under the Curve, "N/A"- Not available

TABLE 12. Source code availability, used hardware and price range for anterior segment imaging - COMPLETE SOLUTIONS.

Solution availability (open/closed source code)	Used Hardware	Estimated price range (hardware)	First author [reference]
No (closed source)	Smartphone camera	-	Baig [27]
No (closed source but available as Android application)	Smartphone camera	-	Bernard [28]
Yes (data available upon request)	New Vision BIO-SLIPS, HAAG-STREIT BQ900/BX900, and Topcon SL-3G slit- lamp microscopes + multiple smartphone cameras	High-end	Chen J [29]
Yes (data available upon request)	Smartphone camera	-	Chen W [30]
No (closed source)	Smartphone-based corneal topographer SmartKC + smartphone camera A medical-grade topographer Optikon Keratron	High-end	Gairola [31]
No (closed source)	Smartphone camera	-	Gupta H [32]
No (closed source)	Smartphone camera	-	Neogi [33]
Yes (public datasets used, closed source)	-	-	Perera [34]
Yes (open source, data available upon request)	Camera-mounted slit-lamp microscopes (Haag-Streit, Zeiss, Takagi) Smartphone camera	High-end	Ueno [35]
No (closed source but available as Android application)	Smartphone camera	-	Vasan [36]
Yes (public datasets used, closed source)	Smartphone camera	-	Verma [37]

* The estimated price does not include the price of the mobile device and is only a rough estimate based on available quotes to three categories: Low-cost equipment (Items priced between $0 and $100 USD), Mid-range equipment (Items priced between $100 and $1,000 USD), High-end equipment (Items priced at $1,000 USD or more).

TABLE 13. Source code availability, used hardware and price range for anterior segment imaging - PARTIAL SOLUTIONS.

Solution availability (open/closed source code)	Used Hardware	Estimated price range (hardware)	First author [reference]
No (closed source)	-	-	Abdani 2020, [38]
No (closed source)	-	-	Abdani 2021, [39]
Yes (public datasets used, open-source implementation)	-	-	Charan [40]
No (closed source)	Smartphone cameras	-	Chen R [41]
No (closed source)	Smartphone camera	-	Chun [42]
No (closed source)	Nikon COOLPIX S8200 16.1 MP CMOS Digital Camera	Mid-range	De Figueiredo [43]
No (closed source)	Smartphone camera	-	Hong [44]
No (closed source)	Custom smartphone-based slit-lamps.	Mid-range	Hu [45]
Yes (open-source implementation + training data)	CANTON OPTICS LS-7 Digital Slit-lamp SANYO VPC-MZ3GX digital camera Kanghua SLM-3 Digital Slit-lamp Nikon D5300 Digital SLR Camera Smartphone camera	High-end	Li Z [46]
Yes (data available upon request)	Digital Slit-lamp Smartphone camera	High-end	Liu [48]
Yes (data available upon request)	oDocs Nun IR fundus camera	High-end	Linde [47]
Yes (public datasets used, open source and available as web-based application)	Haag-Streit BX 900 LED Slit Lamp	High-end	Long [49]
Yes (public datasets used, closed source)	Single-lens reflex (SLR) camera with a macro lens	Mid-range	Milad [50]
Yes (open-source implementation + training data)	Digital and smartphone cameras	Mid-range	Mukherjee [51]
No (closed source)	Smartphone camera + ambient light	Low-cost	Murali [52]
Yes (public datasets used, closed source)	-	-	Nair [53]
No (closed source)	Smartphone camera + grid-like cylinder with ring light	Low-cost	Okazaki [54]
Yes (training data only, closed source)	Haag Streit Biometer Lenstar LS-900 (for measurements) + smartphone attached to a slit lamp by smartphone adapter	High-end	Qian [55]
No (closed source)	Smartphone camera	-	Ramlan [56]
Yes (open source)	Canon EOS 77D camera with Canon EF 100 mm f/2.8 Macro USM prime lens and MR-14EX macro ring lite flash	Mid-range	Van Brummen [57]
Yes (training data only, closed source)	KangHua SLM-6E and SLM-3 slit lamps equipped with Nikon DSC D5200 and a SANYO VPC-MZ3GX cameras + Smartphone cameras attached to the lamp eyepiece	High-end	Wang [58]
Yes (training data only, closed source)	Smartphone camera	-	Yoo [59]
No (closed source)	OCULUS Easygraph Topographer (for measurements) + Smartphone camera	High-end	Zaki [60]

* The estimated price does not include the price of the mobile device and is only a rough estimate based on available quotes to three categories: Low-cost equipment (Items priced between $0 and $100 USD), Mid-range equipment (Items priced between $100 and $1,000 USD), High-end equipment (Items priced at $1,000 USD or more).

TABLE 14. Source code availability, used hardware and price range for posterior segment imaging - COMPLETE SOLUTIONS.

Solution availability (open/closed source code)	Used Hardware	Estimated price range (hardware)	First author [reference]
No (closed source)	Remidio Fundus On Phone Non-Mydriatic device FOP NM-10 for retinal imaging + smartphone camera	High-end	Jain [62] Kemp [63] Natarajan [61] Sosale [10]
No (closed source)	Remidio Fundus On Phone Non-Mydriatic device FOP NM-10 for retinal imaging + smartphone camera	High-end	Rao [64] Shroff [65]
No (closed source)	Remidio Fundus On Phone Non-Mydriatic device FOP NM-10 for retinal imaging + smartphone camera	High-end	Rajalakshmi [66]
No (closed source)	Custom portable device for retinal imaging + smartphone camera	Mid-range	Kim T [67]
Yes (public datasets used, closed source)	Custom 3D printed camera module prototype + smartphone camera	Low-cost	Kim W [68]
Yes (data available upon request)	Phelcom Eyer retinal device + smartphone camera	High-end	Malerbi [69]
No (closed source)	Phelcom Eyer retinal device + smartphone camera	High-end	Penha [70]
No (closed source)	D-EYE device for retinal imaging + smartphone camera	Mid-range	Wei [71]
No (closed source)	Volk Optical iNview Portable + mobile device camera	Mid-range	Elloumi 2022 [72]
No (closed source)	Custom portable device for retinal imaging + smartphone camera	Mid-range	Alves [73]
Yes (public datasets used, closed source)	An external microscopic lens + smartphone camera	Low-cost	Bourouis [74]

* The estimated price does not include the price of the mobile device and is only a rough estimate based on available quotes to three categories: Low-cost equipment (Items priced between $0 and $100 USD), Mid-range equipment (Items priced between $100 and $1,000 USD), High-end equipment (Items priced at $1,000 USD or more).

TABLE 15. Source code availability, used hardware and price range for posterior segment imaging - PARTIAL SOLUTIONS.

Solution availability (open/closed source code)	Used Hardware	Estimated price range (harware)	First author [reference]
Yes (public datasets used, source code available upon request)	-	-	Al-Absi [75]
Yes (public datasets used, closed source)	-	-	Ali [76]
Yes (public datasets used, closed source)	-	-	Bidari [77]
Yes (training data only, closed source)	Panoptic ophthalmoscope Welch Allyn 11820	Mid-range	Braganca [78]
Yes (public datasets used, closed source)	-	-	Elloumi 2021 [79]
Yes (public datasets used, closed source)	-	-	Ghouali [80]
Yes (public datasets used, closed source but available as The Yanbao App – only for data evaluation)	Simple indirect ophthalmoscope + smartphone camera	Mid-range	Guo [81]
Yes (closed source, open hardware – not the original authors)	Custom smartphone fundus camera (DIYretCAM)	Low-cost	Gupta S [82]
No (closed source)	Custom portable device for retinal imaging + smartphone camera	Mid-range	Hagos [83]
Yes (training data only, closed source)	Welch Allyn iExaminer System (PanOptic Ophthalmoscope + iExaminer adapter + smartphone camera)	Mid-range	Hu [84]
Yes (public datasets used, closed source)	-	-	Intaraprasit [85]
Yes (public datasets used, closed source)	-	-	Li YH [86]
No (closed source)	DigiSight Paxos Scope lens attachment + smartphone camera	Mid-range	Ludwig [87]
No (closed source)	RetCam 3 Wide-Field Digital Imaging System	High-end	Luo [88]
No (closed source)	D-EYE device for retinal imaging + smartphone camera	Mid-range	Maddala [89]
No (closed source)	D-EYE device for retinal imaging + smartphone camera	Mid-range	Majumder [90]
Yes (public datasets used, closed source)	-	-	Martins [91]
Yes (public datasets used, closed source)	-	-	Matthew [92]
Yes (public datasets used, closed source)	-	-	Mutua [93]
Yes (public datasets used, closed source)	-	-	Nage [94]
Yes (training data only, closed source)	Kowa nonmyd WX3D fundus camera D-EYE device for retinal imaging + smartphone camera	High-end	Nakahara [95]
No (closed source)	D-EYE device for retinal imaging + smartphone camera	Mid-range	Neto [96]
Yes (public datasets used, closed source)	-	-	Shrimali [97]
No (closed source)	Natus Retcam, Volk 28D BIO Lens + smartphone camera	High-end	Subrammaniam [98]
Yes (public datasets used, closed source)	-	-	Suriyal [99]

* The estimated price does not include the price of the mobile device and is only a rough estimate based on available quotes to three categories: Low-cost equipment (Items priced between $0 and $100 USD), Mid-range equipment (Items priced between $100 and $1,000 USD), High-end equipment (Items priced at $1,000 USD or more).

AUTHORS CONTRIBUTION

V. Kurilova developed the experimental premises, design, and procedures. The division of the reviewed articles into clinical groups and the extraction of technical data was performed by V. Kurilova. N. Majtanova and P. Kolar verified the results. J. Goga, J. Pavlovicova, and M. Oravec analyzed the data and evaluated the results. V. Kurilova and A. Thurzo processed the images. N. Majtanova, V. Kurilova, J. Goga, J. Pavlovicova, M. Oravec, and P. Kolar prepared the manuscript. All authors interpreted the results, contributed to the manuscript revision, and approved the submitted version.

COMPETING INTERESTS

The authors declare no conflict of interest.

REFERENCES

[1] S. Flaxman et al., "Global causes of blindness and distance vision impairment 1990–2020: A systematic review and meta-analysis," *Lancet Global Health*, vol. 5, no. 12, pp. e1221–e1234, Dec. 2017.

[2] Early Treatment Diabetic Retinopathy Study Research Group, "Early photocoagulation for diabetic retinopathy: ETDRS report number 9," *Ophthalmology*, vol. 98, no. 5, pp. 766–785, May 1991.

[3] R. Rauch, B. Weingessel, S. M. Maca, and P. V. Vecsei-Marlovits, "Time to first treatment: The significance of early treatment of exudative age-related macular degeneration," *Retina*, vol. 32, no. 7, pp. 1260–1264, Jul. 2012.

[4] S. W. Chiang and L. A. Al-Aswad, "Artificial intelligence and other applications in ophthalmology and beyond," in *Artificial Intelligence and Ophthalmology: Perks, Perils and Pitfalls* (Current Practices in Ophthalmology), P. Ichhpujani and S. Thakur, Eds., Singapore: Springer, 2021, pp. 113–132, doi: 10.1007/978-981-16-0634-2_9.

[5] *Smartphone Penetration Worldwide*. Accessed: Feb. 15, 2024. [Online]. Available: https://www.statista.com/statistics/203734/global-smartphone-penetration-per-capita-since-2005/

[6] L. B. Williams, S. G. Prakalapakorn, Z. Ansari, and R. Goldhardt, "Impact and trends in global ophthalmology," *Current Ophthalmology Rep.*, vol. 8, no. 3, pp. 136–143, Jun. 2020.

[7] A. Bastawrous, H. K. Rono, I. A. T. Livingstone, H. A. Weiss, S. Jordan, H. Kuper, and M. J. Burton, "Development and validation of a smartphone-based visual acuity test (peek acuity) for clinical practice and community-based fieldwork," *JAMA Ophthalmology*, vol. 133, no. 8, pp. 930–937, Aug. 2015.

[8] L. J. Haddock and C. Qian, "Smartphone technology for fundus photography," *Retinal Physician*, vols. 8–51, no. 8, pp. 51–58, Jun. 2015. [Online]. Available: https://www.retinalphysician.com/issues/2015/june-2015/smartphone-technology-for-fundus-photography

[9] Y.-C. Jheng, Y.-B. Chou, C.-L. Kao, A. A. Yarmishyn, C.-C. Hsu, T.-C. Lin, P.-Y. Chen, Z.-K. Kao, S.-J. Chen, and D.-K. Hwang, "A novelty route for smartphone-based artificial intelligence approach to ophthalmic screening," *J. Chin. Med. Assoc.*, vol. 83, no. 10, pp. 898–899, Oct. 2020.

[10] B. Sosale, A. Sosale, H. Murthy, S. Sengupta, and M. Naveenam, "Medios—An offline, smartphone-based artificial intelligence algorithm for the diagnosis of diabetic retinopathy," *Indian J. Ophthalmol.*, vol. 68, no. 2, p. 391, Feb. 2020.

[11] Vishwanath, D. T. Swamy, and D. S. Gaddi, "Smartphone for retinal imaging–case series in resource-limited rural settings," *Indian J. Ophthalmology*, vol. 71, no. 5, pp. 2008–2013, May 2023.

[12] A. M. Yusuf, R. C. Lusobya, J. Mukisa, C. Batte, D. Nakanjako, and O. Juliet-Sengeri, "Validity of smartphone-based retinal photography (PEEK-retina) compared to the standard ophthalmic fundus camera in diagnosing diabetic retinopathy in uganda: A cross-sectional study," *PLoS ONE*, vol. 17, no. 9, Sep. 2022, Art. no. e0273633.

[13] U. Iqbal, "Smartphone fundus photography: A narrative review," *Int. J. Retina Vitreous*, vol. 7, no. 1, p. 44, Jun. 2021.

[14] A. Pujari, "Smartphone ophthalmoscopy: Is there a place for it?" *Clin. Ophthalmol.*, vol. 15, pp. 4333–4337, Oct. 2021.

[15] S. Das, H. J. Kuht, I. De Silva, S. S. Deol, L. Osman, J. Burns, N. Sarvananthan, U. Sarodia, B. Kapoor, T. Islam, R. Sampath, A. Poyser, V. Konidaris, R. Anzidei, F. A. Proudlock, and M. G. Thomas, "Feasibility and clinical utility of handheld fundus cameras for retinal imaging," *Eye*, vol. 37, no. 2, pp. 274–279, Feb. 2023.

[16] F. Hafiz, R. J. Chalakkal, S. C. Hong, G. Linde, R. Hu, B. O'Keeffe, and Y. Boobin, "A new approach to non-mydriatic portable fundus imaging," *Expert Rev. Med. Devices*, vol. 19, no. 4, pp. 303–314, Apr. 2022.

[17] D. Shah, L. Dewan, A. Singh, D. Jain, T. Damani, R. Pandit, A. C. Porwal, S. Bhatnagar, M. Shrishrimal, and A. Patel, "Utility of a smartphone assisted direct ophthalmoscope camera for a general practitioner in screening of diabetic retinopathy at a primary health care center," *Indian J. Ophthalmology*, vol. 69, no. 11, pp. 3144–3148, Nov. 2021.

[18] A. Singh, K. Cheyne, G. Wilson, M. J. Sime, and S. C. Hong, "On the use of a new monocular-indirect ophthalmoscope for retinal photography in a primary care setting," *New Zealand Med. J.*, vol. 133, no. 1512, pp. 31–38, Apr. 2020.

[19] K. Iyengar, G. K. Upadhyaya, R. Vaishya, and V. Jain, "COVID-19 and applications of smartphone technology in the current pandemic," *Diabetes Metabolic Syndrome, Clin. Res. Rev.*, vol. 14, no. 5, pp. 733–737, Sep. 2020.

[20] S. Zhang, T. B. Tis, and Q. Wei, "Chapter 48—Smartphone-based clinical diagnostics," in *Precision Medicine for Investigators, Practitioners and Providers*, J. Faintuch and S. Faintuch, Eds., New York, NY, USA: Academic, Jan. 2020, ch. 2, pp. 493–508. [Online]. Available: https://www.sciencedirect.com/science/article/pii/B9780128191781000484

[21] R. S. Meshkin, G. W. Armstrong, N. E. Hall, E. J. Rossin, M. B. Hymowitz, and A. C. Lorch, "Effectiveness of a telemedicine program for triage and diagnosis of emergent ophthalmic conditions," *Eye*, vol. 37, no. 2, pp. 325–331, Feb. 2023.

[22] T.-C. Yeh, K.-J. Lo, D.-K. Hwang, T.-C. Lin, and Y.-B. Chou, "Evaluation of a remote telemedicine platform using a novel handheld fundus camera: Physician and patient perceptions from real-world experience," *J. Chin. Med. Assoc.*, vol. 85, no. 7, pp. 793–798, Jul. 2022.

[23] L. Balyen and T. Petõ, "Promising artificial intelligence-machine learning-deep learning algorithms in ophthalmology," *Asia–Pacific J. Ophthalmology*, vol. 8, no. 3, pp. 264–272, Jun. 2019.

[24] S. K. Zhou, H. Greenspan, C. Davatzikos, J. S. Duncan, B. Van Ginneken, A. Madabhushi, J. L. Prince, D. Rueckert, and R. M. Summers, "A review of deep learning in medical imaging: Imaging traits, technology trends, case studies with progress highlights, and future promises," *Proc. IEEE*, vol. 109, no. 5, pp. 820–838, May 2021.

[25] D. S. W. Ting, L. Peng, A. V. Varadarajan, P. A. Keane, P. M. Burlina, M. F. Chiang, L. Schmetterer, L. R. Pasquale, N. M. Bressler, D. R. Webster, M. Abramoff, and T. Y. Wong, "Deep learning in ophthalmology: The technical and clinical considerations," *Prog. Retinal Eye Res.*, vol. 72, Sep. 2019, Art. no. 100759.

[26] G. S. Collins et al., "TRIPOD+AI statement: Updated guidance for reporting clinical prediction models that use regression or machine learning methods," *BMJ*, vol. 385, Apr. 2024, Art. no. e078378. [Online]. Available: https://www.bmj.com/content/385/bmj-2023-078378

[27] M. A. Baig, T. Hussain, M. D. Khan, A. Malik, and F. Akram, "Smartphone-based AI detection of ocular diseases," in *Proc. Int. Conf. IT Ind. Technol. (ICIT)*, Oct. 2023, pp. 1–7. [Online]. Available: https://ieeexplore.ieee.org/abstract/document/10335803?casa_token=O1GM_QV2WbEAAAAA:y81wWL4oEUUR3B7JoWDPCHMJR8Etfs1sVQ8Hs81WeZOWjIyzj_LXFAiNA2S2071mrMMTkbjng5oD

[28] A. Bernard, S. Z. Xia, S. Saleh, T. Ndukwe, J. Meyer, E. Soloway, M. Sintayehu, and B. T. Ramet, "EyeScreen: Development and potential of a novel machine learning application to detect leukocoria," *Ophthalmology Sci.*, vol. 2, no. 3, Sep. 2022, Art. no. 100158.

[29] J. Chen et al., "EE-explorer: A multimodal artificial intelligence system for eye emergency triage and primary diagnosis," *Amer. J. Ophthalmology*, vol. 252, pp. 253–264, Aug. 2023.

[30] W. Chen et al., "Early detection of visual impairment in young children using a smartphone-based deep learning system," *Nature Med.*, vol. 29, no. 2, pp. 493–503, Feb. 2023.

[31] S. Gairola, P. Joshi, A. Balasubramaniam, K. Murali, N. Kwatra, and M. Jain, "Keratoconus classifier for smartphone-based corneal topographer," in *Proc. 44th Annu. Int. Conf. IEEE Eng. Med. Biol. Soc. (EMBC)*, Jul. 2022, pp. 1875–1878.

[32] H. Gupta, "Heterotropia diagnosis with smartphone using machine learning and computer vision," in *Proc. 3rd Int. Conf. Contemp. Comput. Informat. (IC3I)*, Oct. 2018, pp. 160–165.
[33] D. Neogi, M. A. Chowdhury, M. M. Akter, and M. I. A. Hossain, "Mobile detection of cataracts with an optimised lightweight deep edge intelligent technique," *IET Cyber-Phys. Syst., Theory Appl.*, vol. 9, no. 3, pp. 269–281, Sep. 2024. [Online]. Available: https://onlinelibrary.wiley.com/doi/abs/10.1049/cps2.12083
[34] B. D. K. Perera, W. A. A. I. Wickramarathna, S. Chandrasiri, W. A. P. W. Wanniarachchi, S. H. N. Dilshani, and N. Pemadasa, "UveaTrack: Uveitis eye disease prediction and detection with vision function calculation and risk analysis," in *Proc. IEEE 13th Annu. Inf. Technol., Electron. Mobile Commun. Conf. (IEMCON)*, Oct. 2022, pp. 0088–0093. [Online]. Available: https://ieeexplore.ieee.org/document/9946505
[35] Y. Ueno, M. Oda, T. Yamaguchi, H. Fukuoka, R. Nejima, Y. Kitaguchi, M. Miyake, M. Akiyama, K. Miyata, K. Kashiwagi, N. Maeda, J. Shimazaki, H. Noma, K. Mori, and T. Oshika, "Deep learning model for extensive smartphone-based diagnosis and triage of cataracts and multiple corneal diseases," *Brit. J. Ophthalmology*, vol. 108, no. 10, pp. 1406–1413, Jan. 2024. [Online]. Available: https://bjo.bmj.com/content/early/2024/01/18/bjo-2023-324488
[36] C. S. Vasan, S. Gupta, M. Shekhar, K. Nagu, L. Balakrishnan, R. D. Ravindran, T. Ravilla, and G.-B.-B. Subburaman, "Accuracy of an artificial intelligence-based mobile application for detecting cataracts: Results from a field study," *Indian J. Ophthalmology*, vol. 71, no. 8, pp. 2984–2989, Aug. 2023.
[37] S. Verma, I. Singh, K. Ray, R. Patra, and D. Das, "ICAT: Intelligent cataract detection using deep neural in smartphone," in *Proc. IEEE Int. Women Eng. (WIE) Conf. Electr. Comput. Eng. (WIECON-ECE)*, Dec. 2022, pp. 126–131. [Online]. Available: https://ieeexplore.ieee.org/document/10151127
[38] S. R. Abdani, M. A. Zulkifley, and A. M. Moubark, "Pterygium tissues segmentation using densely connected DeepLab," in *Proc. IEEE 10th Symp. Comput. Appl. Ind. Electron. (ISCAIE)*, Apr. 2020, pp. 229–232.
[39] S. R. Abdani, M. A. Zulkifley, and N. H. Zulkifley, "Group and shuffle convolutional neural networks with pyramid pooling module for automated pterygium segmentation," *Diagnostics*, vol. 11, no. 6, p. 1104, Jun. 2021.
[40] A. Charan, K. Mounav, T. Anuradha, and P. Y. Sai Srinivas, "Automated prediction of cataract disease," in *Proc. Int. Conf. Advancement Comput. Comput. Technol. (InCACCT)*. Gharuan, India: IEEE, May 2023, pp. 191–195. [Online]. Available: https://ieeexplore.ieee.org/document/10141822/
[41] R. Chen, W. Zeng, W. Fan, F. Lai, Y. Chen, X. Lin, L. Tang, W. Ouyang, Z. Liu, and X. Luo, "Automatic recognition of ocular surface diseases on smartphone images using densely connected convolutional networks," in *Proc. 43rd Annu. Int. Conf. IEEE Eng. Med. Biol. Soc. (EMBC)*, Nov. 2021, pp. 2786–2789.
[42] J. Chun, Y. Kim, K. Y. Shin, S. H. Han, S. Y. Oh, T.-Y. Chung, K.-A. Park, and D. H. Lim, "Deep learning–based prediction of refractive error using photorefraction images captured by a smartphone: Model development and validation study," *JMIR Med. Informat.*, vol. 8, no. 5, May 2020, Art. no. e16225.
[43] L. A. de Figueiredo, J. V. P. Dias, M. Polati, P. C. Carricondo, and I. Debert, "Strabismus and artificial intelligence app: Optimizing diagnostic and accuracy," *Translational Vis. Sci. Technol.*, vol. 10, no. 7, p. 22, Jun. 2021.
[44] Y. Hong and M. Hasegawa, "Study of minor dry-eye detection using smartphone camera based on deep learning," in *Proc. Int. Workshop Adv. Imag. Technol. (IWAIT)*, Mar. 2021, pp. 621–626. [Online]. Available: https://www.spiedigitallibrary.org/conference-proceedings-of-spie/11766/1176633/Study-of-minor-dry-eye-detection-using-smartphone-camera-based/10.1117/12.2590408.full
[45] S. Hu, X. Wang, H. Wu, X. Luan, P. Qi, Y. Lin, X. He, and W. He, "Unified diagnosis framework for automated nuclear cataract grading based on smartphone slit-lamp images," *IEEE Access*, vol. 8, pp. 174169–174178, 2020.
[46] Z. Li, J. Jiang, K. Chen, Q. Chen, Q. Zheng, X. Liu, H. Weng, S. Wu, and W. Chen, "Preventing corneal blindness caused by keratitis using artificial intelligence," *Nature Commun.*, vol. 12, no. 1, p. 3738, Jun. 2021.
[47] G. Linde, R. Chalakkal, L. Zhou, J. L. Huang, B. O'Keeffe, D. Shah, S. Davidson, and S. C. Hong, "Automatic refractive error estimation using deep learning-based analysis of red reflex images," *Diagnostics*, vol. 13, no. 17, p. 2810, Aug. 2023.
[48] Y. Liu, C. Xu, S. Wang, Y. Chen, X. Lin, S. Guo, Z. Liu, Y. Wang, H. Zhang, Y. Guo, C. Huang, H. Wu, Y. Li, Q. Chen, J. Hu, Z. Luo, and Z. Liu, "Accurate detection and grading of pterygium through smartphone by a fusion training model," *Brit. J. Ophthalmology*, vol. 108, no. 3, pp. 336–342, Mar. 2024.
[49] E. Long et al., "Artificial intelligence manages congenital cataract with individualized prediction and telehealth computing," *NPJ Digit. Med.*, vol. 3, no. 1, p. 112, Aug. 2020.
[50] D. Milad, F. Antaki, M.-C. Robert, and R. Duval, "Development and deployment of a smartphone application for diagnosing trachoma: Leveraging code-free deep learning and edge artificial intelligence," *Saudi J. Ophthalmology*, vol. 37, no. 3, pp. 200–206, Jul. 2023. [Online]. Available: https://journals.lww.com/sjop/fulltext/2023/37030/development_and_deployment_of_a_smartphone.6.aspx
[51] P. Mukherjee, I. Bhattacharyya, M. Mullick, R. Kumar, N. D. Roy, and M. Mahmud, "iConDet: An intelligent portable healthcare app for the detection of conjunctivitis," in *Applied Intelligence and Informatics* (Communications in Computer and Information Science), M. Mahmud, M. S. Kaiser, N. Kasabov, K. Iftekharuddin, and N. Zhong, Eds., Cham, Switzerland: Springer, 2021, pp. 29–42.
[52] K. Murali, V. Krishna, V. Krishna, and B. Kumari, "Application of deep learning and image processing analysis of photographs for amblyopia screening," *Indian J. Ophthalmology*, vol. 68, no. 7, p. 1407, Jul. 2020.
[53] S. V. Nair and P. Shete, "Mobile application for cataract detection using convolution neural network," in *Proc. Int. Conf. Netw., Multimedia Inf. Technol. (NMITCON)*, Sep. 2023, pp. 1–6. [Online]. Available: https://ieeexplore.ieee.org/abstract/document/10276326?casa_token=sXJcEiZG7TIAAAAA:QBJleNFTCF6KR9wt8T88_8yabT4_6sPW7q1ZyyCDVm_6AUgEsuGp_Sz3fcLrQ01eIOQh1EtL-5wJ
[54] K. Okazaki and M. Hasegawa, "Proposal for dry eye detection caused by contact lenses using a smartphone with a ring light and deep learning technology," in *Proc. Int. Tech. Conf. Circuits/Systems, Comput., Commun. (ITC-CSCC)*, Jun. 2023, pp. 1–5. [Online]. Available: https://ieeexplore.ieee.org/document/10212584/
[55] C. Qian, Y. Jiang, Z. D. Soh, G. S. Selvam, S. Xiao, Y. C. Tham, X. Xu, Y. Liu, J. Li, H. Zhong, and C. Cheng, "Smartphone-acquired anterior segment images for deep learning prediction of anterior chamber depth: A proof-of-concept study," in *Proc. Frontiers Med.*, vol. 9, Jun. 2022. [Online]. Available: https://www.frontiersin.org/journals/medicine/articles/10.3389/fmed.2022.912214/full
[56] L. A. Ramlan, W. M. D. W. Zaki, H. A. Mutalib, A. Hussain, and A. Mustapha, "Cataract detection using pupil patch classification and ruled-based system in anterior segment photographed images," in *Proc. IEEE 13th Symp. Comput. Appl. Ind. Electron. (ISCAIE)*. Penang, Malaysia: IEEE, May 2023, pp. 124–129. [Online]. Available: https://ieeexplore.ieee.org/document/10165004/
[57] A. Van Brummen, J. P. Owen, T. Spaide, C. Froines, R. Lu, M. Lacy, M. Blazes, E. Li, C. S. Lee, A. Y. Lee, and M. Zhang, "PeriorbitAI: Artificial intelligence automation of eyelid and periorbital measurements," *Amer. J. Ophthalmology*, vol. 230, pp. 285–296, Oct. 2021.
[58] L. Wang, K. Chen, H. Wen, Q. Zheng, Y. Chen, J. Pu, and W. Chen, "Feasibility assessment of infectious keratitis depicted on slit-lamp and smartphone photographs using deep learning," *Int. J. Med. Informat.*, vol. 155, Nov. 2021, Art. no. 104583.
[59] T. K. Yoo, J. Y. Choi, H. K. Kim, I. H. Ryu, and J. K. Kim, "Adopting low-shot deep learning for the detection of conjunctival melanoma using ocular surface images," *Comput. Methods Programs Biomed.*, vol. 205, Jun. 2021, Art. no. 106086.
[60] W. M. D. W. Zaki, M. M. Daud, A. H. Saad, A. Hussain, and H. A. Mutalib, "Towards automated keratoconus screening approach using lateral segment photographed images," in *Proc. IEEE-EMBS Conf. Biomed. Eng. Sci. (IECBES)*, Mar. 2021, pp. 466–471.
[61] S. Natarajan, A. Jain, R. Krishnan, A. Rogye, and S. Sivaprasad, "Diagnostic accuracy of community-based diabetic retinopathy screening with an offline artificial intelligence system on a smartphone," *JAMA Ophthalmology*, vol. 137, no. 10, pp. 1182–1188, Oct. 2019.
[62] A. Jain, R. Krishnan, A. Rogye, and S. Natarajan, "Use of offline artificial intelligence in a smartphone-based fundus camera for community screening of diabetic retinopathy," *Indian J. Ophthalmology*, vol. 69, no. 11, pp. 3150–3154, Nov. 2021.
[63] O. Kemp, C. Bascaran, E. Cartwright, L. McQuillan, N. Matthew, H. Shillingford-Ricketts, M. Zondervan, A. Foster, and M. Burton, "Real-world evaluation of smartphone-based artificial intelligence to screen for diabetic retinopathy in dominica: A clinical validation study," *BMJ Open Ophthalmology*, vol. 8, no. 1, Dec. 2023, Art. no. e001491.

[64] D. P. Rao, S. Shroff, F. M. Savoy, S. Shruthi, C. Hsu, K. Negiloni, Z. S. Pradhan, P. V. Jayasree, A. Sivaraman, and H. L. Rao, "Evaluation of an offline, artificial intelligence system for referable glaucoma screening using a smartphone-based fundus camera: A prospective study," *Eye*, vol. 38, no. 6, pp. 1104–1111, Dec. 2023.

[65] S. Shroff, D. P. Rao, F. M. Savoy, S. Shruthi, C.-K. Hsu, Z. S. Pradhan, P. V. Jayasree, A. Sivaraman, S. Sengupta, R. Shetty, and H. L. Rao, "Agreement of a novel artificial intelligence software with optical coherence tomography and manual grading of the optic disc in glaucoma," *J. Glaucoma*, vol. 32, no. 4, pp. 280–286, Apr. 2023.

[66] R. Rajalakshmi, R. Subashini, R. M. Anjana, and V. Mohan, "Automated diabetic retinopathy detection in smartphone-based fundus photography using artificial intelligence," *Eye*, vol. 32, no. 6, pp. 1138–1144, Jun. 2018.

[67] T. N. Kim, M. T. Aaberg, P. Li, J. R. Davila, M. Bhaskaranand, S. Bhat, C. Ramachandra, K. Solanki, F. Myers, C. Reber, R. Jalalizadeh, T. P. Margolis, D. Fletcher, and Y. M. Paulus, "Comparison of automated and expert human grading of diabetic retinopathy using smartphone-based retinal photography," *Eye*, vol. 35, no. 1, pp. 334–342, Jan. 2021.

[68] W. Kim, "The implementation of ocular health service system using Android platform," *J. ICT Standardization*, vol. 10, no. 3, pp. 427–438, Aug. 2022. [Online]. Available: https://journals.riverpublishers.com/index.php/JICTS

[69] F. K. Malerbi, R. E. Andrade, P. H. Morales, J. A. Stuchi, D. Lencione, J. V. de Paulo, M. P. Carvalho, F. S. Nunes, R. M. Rocha, D. A. Ferraz, and R. Belfort, "Diabetic retinopathy screening using artificial intelligence and handheld smartphone-based retinal camera," *J. Diabetes Sci. Technol.*, vol. 16, no. 3, pp. 716–723, May 2022.

[70] F. M. Penha, B. M. Priotto, F. Hennig, B. Przysiezny, B. A. Wiethorn, J. Orsi, I. B. F. Nagel, B. Wiggers, J. A. Stuchi, D. Lencione, P. V. de Souza Prado, F. Yamanaka, F. Lojudice, and F. K. Malerbi, "Single retinal image for diabetic retinopathy screening: Performance of a handheld device with embedded artificial intelligence," *Int. J. Retina Vitreous*, vol. 9, no. 1, p. 41, Jul. 2023.

[71] H. Wei, A. Sehgal, and N. Kehtarnavaz, "A deep learning-based smartphone app for real-time detection of retinal abnormalities in fundus images," in *Proc. Real-Time Image Process. Deep Learn.*, May 2019, p. 1. [Online]. Available: https://www.spiedigitallibrary.org/conference-proceedings-of-spie/10996/1099602/A-deep-learning-based-smartphone-app-for-real-time-detection/10.1117/12.2516665.full

[72] Y. Elloumi, N. Abroug, and M. H. Bedoui, "End-to-end mobile system for diabetic retinopathy screening based on lightweight deep neural network," in *Advances in Intelligent Data Analysis XX* (Lecture Notes in Computer Science), T. Bouadi, E. Fromont, and E. Hüllermeier, Eds., Cham, Switzerland: Springer, 2022, pp. 66–77.

[73] S. S. A. Alves, A. G. Matos, J. S. Almeida, C. A. Benevides, C. C. H. Cunha, R. V. C. Santiago, R. F. Pereira, and P. P. Reboucas Filho, "A new strategy for the detection of diabetic retinopathy using a smartphone app and machine learning methods embedded on cloud computer," in *Proc. IEEE 33rd Int. Symp. Computer-Based Med. Syst. (CBMS)*, Jul. 2020, pp. 542–545.

[74] A. Bourouis, M. Feham, M. A. Hossain, and L. Zhang, "An intelligent mobile based decision support system for retinal disease diagnosis," *Decis. Support Syst.*, vol. 59, pp. 341–350, Mar. 2014.

[75] H. R. H. Al-Absi, G. N. Muchori, S. Musleh, M. T. Islam, A. Pai, and T. Alam, "DMEgrader: Android mobile application for diabetic macular edema grading prediction," in *Proc. Int. Conf. Inf. Technol. (ICIT)*, Aug. 2023, pp. 190–195. [Online]. Available: https://ieeexplore.ieee.org/document/10225808

[76] S. Ali and S. Raut, "Automatic detection of pathological myopia using smartphone app," in *Proc. Int. Conf. Comput. Sci. Comput. Intell. (CSCI)*. Las Vegas, NV, USA: IEEE, Dec. 2022, pp. 406–408. [Online]. Available: https://ieeexplore.ieee.org/document/10216662/

[77] I. Bidari, S. Chickerur, A. Kulkarni, A. Mahajan, A. Nikkam, and A. THM, "Deploying machine learning inference on diabetic retinopathy in binary and multi-class classification," in *Proc. Int. Conf. Ind. Electron. Res. Appl. (ICIERA)*, Dec. 2021, pp. 1–6. [Online]. Available: https://ieeexplore.ieee.org/document/9726533

[78] C. P. Bragança, J. M. Torres, C. P. D. A. Soares, and L. O. Macedo, "Detection of glaucoma on fundus images using deep learning on a new image set obtained with a smartphone and handheld ophthalmoscope," *Healthcare*, vol. 10, no. 12, p. 2345, Nov. 2022.

[79] Y. Elloumi, "Mobile aided system of deep-learning based cataract grading from fundus images," in *Artificial Intelligence in Medicine* (Lecture Notes in Computer Science), A. Tucker, P. H. Abreu, J. Cardoso, P. P. Rodrigues, and D. Riaño, Eds., Cham, Switzerland: Springer, 2021, pp. 355–360.

[80] S. Ghouali, EM. Onyema, MS. Guellil, M. A. Wajid, O. Clare, W. Cherifi, and M. Feham, "Artificial intelligence-based teleopthalmology application for diagnosis of diabetics retinopathy," *IEEE Open J. Eng. Med. Biol.*, vol. 3, pp. 124–133, 2022.

[81] F. Guo, Y. Mai, X. Zhao, X. Duan, Z. Fan, B. Zou, and B. Xie, "Yanbao: A mobile app using the measurement of clinical parameters for glaucoma screening," *IEEE Access*, vol. 6, pp. 77414–77428, 2018.

[82] S. Gupta, S. Thakur, and A. Gupta, "Optimized hybrid machine learning approach for smartphone based diabetic retinopathy detection," *Multimedia Tools Appl.*, vol. 81, no. 10, pp. 14475–14501, Apr. 2022.

[83] M. T. Hagos, S. Kant, and S. A. Bala, "Automated smartphone based system for diagnosis of diabetic retinopathy," in *Proc. Int. Conf. Comput., Commun., Intell. Syst. (ICCCIS)*, Oct. 2019, pp. 256–261.

[84] H. Hu, H. Wei, M. Xiao, L. Jiang, H. Wang, H. Jiang, T. Rundek, and J. Wang, "Characterization of the retinal vasculature in fundus photos using the PanOptic iExaminer system," *Eye Vis.*, vol. 7, no. 1, p. 46, Sep. 2020.

[85] P. Intaraprasit, T. H. Bui, and M. P. Paing, "MobileNetV2-based deep learning for retinal disease classification on a mobile application," in *Proc. 15th Biomed. Eng. Int. Conf. (BMEiCON)*, Oct. 2023, pp. 1–5. [Online]. Available: https://ieeexplore.ieee.org/document/10322079

[86] Y.-H. Li, N.-N. Yeh, S.-J. Chen, and Y.-C. Chung, "Computer-assisted diagnosis for diabetic retinopathy based on fundus images using deep convolutional neural network," *Mobile Inf. Syst.*, vol. 2019, pp. 1–14, Jan. 2019.

[87] C. A. Ludwig, C. Perera, D. Myung, M. A. Greven, S. J. Smith, R. T. Chang, and T. Leng, "Automatic identification of referral-warranted diabetic retinopathy using deep learning on mobile phone images," *Translational Vis. Sci. Technol.*, vol. 9, no. 2, p. 60, Dec. 2020.

[88] Z. Luo, X. Ding, N. Hou, and J. Wan, "A deep-learning-based collaborative edge–cloud telemedicine system for retinopathy of prematurity," *Sensors*, vol. 23, no. 1, p. 276, Dec. 2022.

[89] S. Maddala, K. Nara, S. D. Yerrarapu, and S. Vanam, "Classification of fundus images captured using D-eye smartphone retinal imaging system," in *Proc. Int. Conf. Emerg. Trends Comput. Eng. Appl. (ETCEA)*, Nov. 2022, pp. 1–7. [Online]. Available: https://ieeexplore.ieee.org/document/10009691

[90] S. Majumder, Y. Elloumi, M. Akil, R. Kachouri, and N. Kehtarnavaz, "A deep learning-based smartphone app for real-time detection of five stages of diabetic retinopathy," in *Proc. Real-Time Image Process. Deep Learn.*, Apr. 2020, pp. 13–22. [Online]. Available: https://www.spiedigitallibrary.org/conference-proceedings-of-spie/11401/1140106/A-deep-learning-based-smartphone-app-for-real-time-detection/10.1117/12.2557554.full

[91] J. Martins, J. S. Cardoso, and F. Soares, "Offline computer-aided diagnosis for glaucoma detection using fundus images targeted at mobile devices," *Comput. Methods Programs Biomed.*, vol. 192, Aug. 2020, Art. no. 105341.

[92] A. Matthew, A. A. S. Gunawan, and F. I. Kurniadi, "Diabetic retinopathy diagnosis system based on retinal biomarkers using EfficientNet-B0 for Android devices," in *Proc. IEEE Int. Conf. Commun., Netw. Satell. (COMNETSAT)*, Nov. 2023, pp. 207–212. [Online]. Available: https://ieeexplore.ieee.org/abstract/document/10420736

[93] E. N. Mutua, B. S. Kasamani, and C. Reich, "Smartphone fundus photography enhancement for retinopathy of prematurity disease diagnosis using deep learning," in *Proc. 6th Int. Conf. Comput. Informat. Eng. (IC2IE)*, Sep. 2023, pp. 101–108. [Online]. Available: https://ieeexplore.ieee.org/document/10331154

[94] P. Nage, A. Pandit, S. Jeurkar, and S. Shitole, "Diabetic retinopathy detection using Android application," in *Proc. IEEE Bombay Sect. Signature Conf. (IBSSC)*, Dec. 2022, pp. 1–6. [Online]. Available: https://ieeexplore.ieee.org/abstract/document/10037368

[95] K. Nakahara, R. Asaoka, M. Tanito, N. Shibata, K. Mitsuhashi, Y. Fujino, M. Matsuura, T. Inoue, K. Azuma, R. Obata, and H. Murata, "Deep learning-assisted (automatic) diagnosis of glaucoma using a smartphone," *Brit. J. Ophthalmology*, vol. 106, no. 4, pp. 587–592, Apr. 2022.

[96] A. Neto, J. Camara, and A. Cunha, "Evaluations of deep learning approaches for glaucoma screening using retinal images from mobile device," *Sensors*, vol. 22, no. 4, p. 1449, Feb. 2022.

[97] S. Shrimali, "Image filtering and utilization of deep learning algorithms to detect the severity of diabetic retinopathy," in *Proc. IEEE 12th Int. Conf. Commun. Syst. Netw. Technol. (CSNT)*, Apr. 2023, pp. 202–207. [Online]. Available: https://ieeexplore.ieee.org/document/10134680

[98] A. Subramaniam, M. Douglass, F. Orge, B. Can, G. A. Monteoliva, E. Fried, V. Schbib, G. Saidman, B. Peña, S. Ulacia, P. Acevedo, and D. Wilson, "Vessel enhancement in smartphone fundus images to aid retinopathy of prematurity and plus disease diagnosis and classification," in *Proc. SPIE*, vol. 12037, Apr. 2022, p. 5. [Online]. Available: https://www.spiedigitallibrary.org/conference-proceedings-of-spie/12037/1203706/Vessel-enhancement-in-smartphone-fundus-images-to-aid-retinopathy-of/10.1117/12.2613268.full

[99] S. Suriyal, C. Druzgalski, and K. Gautam, "Mobile assisted diabetic retinopathy detection using deep neural network," in *Proc. Global Med. Eng. Phys. Exchanges/Pan Amer. Health Care Exchanges (GMEPE/PAHCE)*, Mar. 2018, pp. 1–4. [Online]. Available: https://ieeexplore.ieee.org/document/8400760

[100] B. Raju, N. Raju, J. Akkara, and A. Pathengay, "Do it yourself smartphone fundus camera—DIYretCAM," *Indian J. Ophthalmology*, vol. 64, no. 9, p. 663, Sep. 2016.

[101] *Digital Retinal Camera | The Direct Ophthalmoscope for Your IPhone | Portable Digital Retinal Camera | D-EYE*. Accessed: Apr. 6, 2024. [Online]. Available: https://www.d-eyecare.com/

[102] Volk Optical. *INview®*. Accessed: Apr. 6, 2024. [Online]. Available: https://www.volk.com/products/inview-for-iphone-6-6s

[103] *Remidio NM Fundus on Phone*. Accessed: Apr. 6, 2024. [Online]. Available: https://www.remidio.us/fop.php

[104] P. Viola and M. Jones, "Rapid object detection using a boosted cascade of simple features," in *Proc. IEEE Comput. Soc. Conf. Comput. Vis. Pattern Recognit. (CVPR)*, vol. 1. Kauai, HI, USA: IEEE Comput. Soc, Dec. 2001, pp. I-511–I-518. [Online]. Available: http://ieeexplore.ieee.org/document/990517/

[105] R. Keshari, S. Ghosh, A. Agarwal, R. Singh, and M. Vatsa, "Mobile periocular matching with pre-post cataract surgery," in *Proc. IEEE Int. Conf. Image Process. (ICIP)*, Sep. 2016, pp. 3116–3120. [Online]. Available: https://ieeexplore.ieee.org/document/7532933

[106] M. Karthik and D. Sohier. (2019). *APTOS 2019 Blindness Detection*. [Online]. Available: https://kaggle.com/competitions/aptos2019-blindness-detection

[107] EyePACS. (2015). *Diabetic Retinopathy Detection*. [Online]. Available: https://www.kaggle.com/c/diabetic-retinopathy-detection

[108] T. Kauppi, V. Kalesnykiene, J.-K. Kamarainen, L. Lensu, I. Sorri, H. Uusitalo, H. Kalviainen, and J. Pietila, "DIARETDB 0: Evaluation database and methodology for diabetic retinopathy algorithms," Mach. Vis. Pattern Recognit. Res. Group, Lappeenranta Univ. Technol., Finland, pp. 1–17, 2007, no. 73.

[109] (2014). *Drishti-GS—Retina dataset for ONH segmentation*. [Online]. Available: http://cvit.iiit.ac.in/projects/mip/drishti-gs/mip-dataset2/Home.php

[110] A. Budai, R. Bock, A. Maier, J. Hornegger, and G. Michelson, "Robust vessel segmentation in fundus images," *Int. J. Biomed. Imag.*, vol. 2013, Oct. 2013, Art. no. 154860.

[111] P. Porwal. (Apr. 2018). *Indian Diabetic Retinopathy Image Dataset (IDRiD)*. [Online]. Available: https://ieee-dataport.org/open-access/indian-diabetic-retinopathy-image-dataset-idrid

[112] *Kaggle Cataract Dataset*. Accessed: Feb. 17, 2024. [Online]. Available: https://www.kaggle.com/datasets/jr2ngb/cataractdataset

[113] E. Decencière, X. Zhang, G. Cazuguel, B. Lay, B. Cochener, C. Trone, P. Gain, R. Ordonez, P. Massin, A. Erginay, B. Charton, and J.-C. Klein, "Feedback on a publicly distributed image database: The messidor database," *Image Anal. Stereology*, vol. 33, no. 3, p. 231, Aug. 2014.

[114] (2019). *Peking University International Competition on Ocular Disease Intelligent Recognition (ODIR-2019)*. [Online]. Available: https://odir2019.grand-challenge.org/

[115] Z. Zhang, F. S. Yin, J. Liu, W. K. Wong, N. M. Tan, B. H. Lee, J. Cheng, and T. Y. Wong, "ORIGA-light: An online retinal fundus image database for glaucoma analysis and research," in *Proc. Annu. Int. Conf. IEEE Eng. Med. Biol.*, Aug. 2010, pp. 3065–3068.

[116] H. Fu. (Jul. 2019). *PALM: PAthoLogic Myopia Challenge*. [Online]. Available: https://ieee-dataport.org/documents/palm-pathologic-myopia-challenge

[117] (2018). *REFUGE–Retina Fundus Glaucoma Challenge*. [Online]. Available: https://refuge.grand-challenge.org/Home2018/

[118] A. Almazroa, S. Alodhayb, E. Osman, E. Ramadan, M. Hummadi, M. Dlaim, M. Alkatee, K. Raahemifar, and V. Lakshminarayanan, "Retinal fundus images for glaucoma analysis: The RIGA dataset," in *Proc. SPIE*, vol. 10579, Mar. 2018, pp. 55–62. [Online]. Available: https://www.spiedigitallibrary.org/conference-proceedings-of-spie/10579/105790B/Retinal-fundus-images-for-glaucoma-analysis-the-RIGA-dataset/10.1117/12.2293584.full

[119] F. Fumero, J. Sigut, S. Alayón, M. González-Hernández, and M. Rosa, "Interactive tool and database for optic disc and cup segmentation of stereo and monocular retinal fundus images," in *Proc. WSCG Conf. Comput. Graph., Vis. Comput. Vis.*, Plzen, Czech Republic, Jun. 2015, pp. 91–97.

[120] M. Vitek, P. Rot, V. Štruc, and P. Peer, "A comprehensive investigation into sclera biometrics: A novel dataset and performance study," *Neural Comput. Appl.*, vol. 32, no. 24, pp. 17941–17955, Dec. 2020, doi: 10.1007/s00521-020-04782-1.

[121] A. W. Hoover and M. Goldbaum. (1999). *STARE (Structured Analysis of the Retina)*. [Online]. Available: https://cecas.clemson.edu/~ahoover/stare/

[122] K. J. Zuiderveld, "Contrast limited adaptive histogram equalization," in *Graphics Gems IV*. New York, NY, USA: Academic, Aug. 1994, pp. 474–485.

[123] A. G. Howard, M. Zhu, B. Chen, D. Kalenichenko, W. Wang, T. Weyand, M. Andreetto, and H. Adam, "MobileNets: Efficient convolutional neural networks for mobile vision applications," 2017, *arXiv:1704.04861*.

[124] X. Zhang, X. Zhou, M. Lin, and J. Sun, "ShuffleNet: An extremely efficient convolutional neural network for mobile devices," in *Proc. IEEE/CVF Conf. Comput. Vis. Pattern Recognit.*, Jun. 2018, pp. 6848–6856. [Online]. Available: https://openaccess.thecvf.com/content_cvpr_2018/html/Zhang_ShuffleNet_An_Extremely_CVPR_2018_paper.html

[125] A. K. Irphan and A. Punitha, "Comparative analysis of ResNet, MobileNet, and EfficientNet models for lung nodule detection and classification," *Int. J. Recent Innov. Trends Comput. Commun.*, vol. 11, no. 11, pp. 1405–1412, 2023. [Online]. Available: https://ijritcc.org/index.php/ijritcc/article/view/10818

[126] S. Han, H. Mao, and W. J. Dally, "Deep compression: Compressing deep neural networks with pruning, trained quantization and Huffman coding," 2015, *arXiv:1510.00149*.

[127] P. Mach and Z. Becvar, "Mobile edge computing: A survey on architecture and computation offloading," *IEEE Commun. Surveys Tuts.*, vol. 19, no. 3, pp. 1628–1656, 3rd Quart., 2017. [Online]. Available: https://ieeexplore.ieee.org/abstract/document/7879258

[128] O. Ali, H. Ali, S. A. A. Shah, and A. Shahzad, "Implementation of a modified U-Net for medical image segmentation on edge devices," *IEEE Trans. Circuits Syst. II, Exp. Briefs*, vol. 69, no. 11, pp. 4593–4597, Nov. 2022. [Online]. Available: https://ieeexplore.ieee.org/abstract/document/9790862

[129] Y. Cai, H. Li, G. Yuan, W. Niu, Y. Li, X. Tang, B. Ren, and Y. Wang, "YOLObile: Real-time object detection on mobile devices via compression-compilation co-design," in *Proc. AAAI Conf. Artif. Intell.*, May 2021, vol. 35, no. 2, pp. 955–963. [Online]. Available: https://ojs.aaai.org/index.php/AAAI/article/view/16179

[130] O. Russakovsky, J. Deng, H. Su, J. Krause, S. Satheesh, S. Ma, Z. Huang, A. Karpathy, A. Khosla, M. Bernstein, A. C. Berg, and L. Fei-Fei, "ImageNet large scale visual recognition challenge," 2014, *arXiv:1409.0575*.

[131] A. Das, P. Rad, K.-K.-R. Choo, B. Nouhi, J. Lish, and J. Martel, "Distributed machine learning cloud teleophthalmology IoT for predicting AMD disease progression," *Future Gener. Comput. Syst.*, vol. 93, pp. 486–498, Apr. 2019.

[132] *Keras: Deep Learning for Humans*. Accessed: Feb. 17, 2024. [Online]. Available: https://keras.io/

[133] Age-Related Eye Disease Study Research Group, "A randomized, placebo-controlled, clinical trial of high-dose supplementation with vitamins C and E, beta carotene, and zinc for age-related macular degeneration and vision loss: AREDS report, no. 8," *Arch. Ophthalmology*, vol. 119, no. 10, pp. 1417–1436, Oct. 2001, doi: 10.1001/archopht.119.10.1417.

[134] L Shanggong Medical Technology Co. *Ocular Disease Recognition*. Accessed: Feb. 17, 2024. [Online]. Available: https://www.kaggle.com/datasets/andrewmvd/ocular-disease-recognition-odir5k
[135] D. Avidor, A. Loewenstein, M. Waisbourd, and A. Nutman, "Cost-effectiveness of diabetic retinopathy screening programs using telemedicine: A systematic review," *Cost Effectiveness Resource Allocation*, vol. 18, no. 1, p. 16, Dec. 2020.
[136] S. Ortiz-Toquero, G. Aleixandre, Y. Valpuesta, C. Perez Fernandez, P. de la Iglesia, J. C. Pastor, and M. Lopez-Galvez, "Cost-effectiveness of a telemedicine optometric-based assessment for screening diabetic retinopathy in a country with a universal public health system," *Telemedicine e-Health*, vol. 30, no. 12, pp. 2824–2833, Dec. 2024. [Online]. Available: https://www.liebertpub.com/doi/10.1089/tmj.2024.0353
[137] X.-M. Huang, B.-F. Yang, W.-L. Zheng, Q. Liu, F. Xiao, P.-W. Ouyang, M.-J. Li, X.-Y. Li, J. Meng, T.-T. Zhang, Y.-H. Cui, and H.-W. Pan, "Cost-effectiveness of artificial intelligence screening for diabetic retinopathy in rural China," *BMC Health Services Res.*, vol. 22, no. 1, p. 260, Feb. 2022, doi: 10.1186/s12913-022-07655-6.
[138] J. D. Gobbi, J. P. R. Braga, M. M. Lucena, V. C. F. Bellanda, M. V. S. Frasson, D. Ferraz, V. Koh, and R. Jorge, "Efficacy of smartphone-based retinal photography by undergraduate students in screening and early diagnosing diabetic retinopathy," *Int. J. Retina Vitreous*, vol. 8, no. 1, p. 35, Jun. 2022, doi: 10.1186/s40942-022-00388-y.
[139] M. A. Zulkifley, S. R. Abdani, and N. H. Zulkifley, "PterygiumNet: A deep learning approach to pterygium detection and localization," *Multimedia Tools Appl.*, vol. 78, no. 24, pp. 34563–34584, Dec. 2019.
[140] M. C. Kim, K. Okada, A. M. Ryner, A. Amza, Z. Tadesse, S. Y. Cotter, B. D. Gaynor, J. D. Keenan, T. M. Lietman, and T. C. Porco, "Sensitivity and specificity of computer vision classification of eyelid photographs for programmatic trachoma assessment," *PLoS ONE*, vol. 14, no. 2, Feb. 2019, Art. no. e0210463. [Online]. Available: https://journals.plos.org/plosone/article?id=10.1371/journal.pone.0210463

V. KURILOVA received the M.D. degree from the Faculty of Medicine, Comenius University, Bratislava, the specialization degree in ophthalmology from the Faculty of Medicine, Slovak Medical University, Bratislava, and the Ph.D. degree in applied informatics from the Slovak University of Technology, where she focused on applying deep learning methods to ophthalmologic images. She is also a Fellow of the European Board of Ophthalmology. She works as a Doctor and a specialist Lecturer at the Department of Ophthalmology, Faculty of Medicine, Slovak Medical University. Her research interests include digital signal and image processing, computer vision, artificial intelligence, neural networks, and machine learning.

J. GOGA received the M.Sc. and Ph.D. degrees in the field of cybernetics in 2017 and 2023, respectively. He is currently a Research Fellow at the Slovak University of Technology, Bratislava. Since 2023, he has been a Research Fellow with the Institute of Robotics and Cybernetics (IRC), Faculty of Electrical Engineering and Information Technology, the Slovak University of Technology. His research interests include artificial neural networks, computer vision, and biometrics.

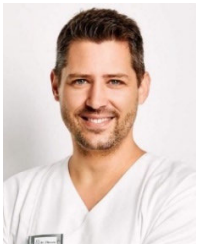

A. THURZO received the M.D. degree with a specialization in dentistry from Comenius University in 2006, the Ph.D. degree from Univerzita Komenského v Bratislave Lekárska Fakulta in 2010, the Master of Public Health degree from Slovenská zdravotnícka univerzita in 2013, and the Master of Health Administration in 2014. He is an Associate Professor and the Head of the Department of Orthodontics and Regenerative and Forensic Dentistry at the Faculty of Medicine, Comenius University, Bratislava, Slovakia. From 1998 to 2003, he was a web coordinator for the British Council, Bratislava. From 2004 to 2005, he worked in new digital technology implementation at the Academic Library of the Medical Faculty, Comenius University. He has been a leading orthodontist at the clinic Sangre Azul since 2013 and an Associate Professor since 2022. His research interests include 3D medical printing, bioprinting, artificial intelligence, orthodontics, forensic dentistry, and regenerative medicine.

J. PAVLOVICOVA was born in Slovakia. She received the M.Sc. and Ph.D. degrees in telecommunication engineering in 2002 and 2006 respectively, and the degree in cybernetics from Faculty of Electrical Engineering and Information Technology, Slovak University of Technology (STU), Bratislava, Slovakia, in 2015. Currently, she is the Deputy Director of the Institute of Robotics and Cybernetics at STU, Bratislava. Her professional activities are characterized by involvement in various areas of research., such as digital signal and image processing, computer vision, health informatics, and explainable artificial intelligence.

M. ORAVEC is a Professor at the Institute of Computer Science and Mathematics, Faculty of Electrical Engineering and Information Technology, Slovak University of Technology (STU), Bratislava, Slovakia. His research interests include artificial intelligence, machine learning and neural networks, biometrics, signal processing, and data analysis. He was a Dean of Faculty of Electrical Engineering and Information Technology, STU, from 2015 to 2023.

P. KOLAR received the M.D., Ph.D., specialization degrees from the Faculty of Medicine, Masaryk University, Brno, specializing in ophthalmology. He is a professorship from the Faculty of Medicine, Masaryk University. He is currently the Head of the Department of Ophthalmology at the Faculty of Medicine, Slovak Medical University, Bratislava. His clinical practice focuses on cataract and vitreoretinal surgery, while his research interests include ophthalmology—particularly age-related macular degeneration and diabetic retinopathy—as well as optometry and diabetology. He serves as the President of the Slovak Ophthalmological Society and is an active member of several Slovak and international ophthalmological societies and committees.

N. MAJTANOVA received the M.D. degree from the Faculty of Medicine, Comenius University, Bratislava, the specialization degree in ophthalmology, and the Ph.D. degree from the Faculty of Medicine, Slovak Medical University, Bratislava. She is an Associate Professor of Ophthalmology and the Deputy Head of the Department of Ophthalmology at the Faculty of Medicine, Slovak Medical University. As a surgeon, her expertise includes cataract, glaucoma, and vitreoretinal surgeries. Her research spans the entire field of ophthalmology, with a particular focus on glaucoma. She is a committee member of the Slovak Ophthalmological Society and a member of the Slovak Glaucoma Society.